DLL1- and DLL4-mediated Notch signaling is essential for adult pancreatic islet homeostasis *(running title –Role of Delta ligands in adult pancreas)*

Marina Rubey[1,2,6*], Nirav Florian Chhabra[1,2*], Daniel Gradinger[1,2,7], Adrián Sanz-Moreno[1], Heiko Lickert[2,4,5], Gerhard K. H. Przemeck[1,2], Martin Hrabě de Angelis[1,2,3**]

1 Helmholtz Zentrum München, Institute of Experimental Genetics and German Mouse Clinic, Neuherberg, Germany

2 German Center for Diabetes Research (DZD), Neuherberg, Germany

3 Chair of Experimental Genetics, Centre of Life and Food Sciences, Weihenstephan, Technische Universität München, Freising, Germany

4 Helmholtz Zentrum München, Institute of Diabetes and Regeneration Research and Institute of Stem Cell Research, Neuherberg, Germany

5 Technische Universität München, Medical Faculty, Munich, Germany

6 Present address Marina Rubey: WMC Healthcare GmbH, Munich, Germany

7 Present address Daniel Gradinger: PSI CRO AG, Munich, Germany

*These authors contributed equally

**Corresponding author: Prof. Dr. Martin Hrabě de Angelis, Helmholtz Zentrum München, German Research Center for Environmental Health, Institute of Experimental Genetics, Ingolstädter Landstr.1, 85764 Neuherberg, Germany. Phone: +49-89-3187-3502. Fax: +49-89-3187-3500. E-mail address: hrabe@helmholtz-muenchen.de

Word count – 4088 / Figures – 7

Diabetes Publish Ahead of Print, published online February 6, 2020

Abstract

Genes of the Notch signaling pathway are expressed in different cell types and organs at different time points during embryonic development and adulthood. The Notch ligand Delta-like 1 (DLL1) controls the decision between endocrine and exocrine fates of multipotent progenitors in the developing pancreas, and loss of *Dll1* leads to premature endocrine differentiation. However, the role of Delta-Notch signaling in adult tissue homeostasis is not well understood. Here, we describe the spatial expression pattern of Notch pathway components in adult murine pancreatic islets and show that DLL1 and -4 are specifically expressed in β-cells, whereas JAGGED1 is expressed in α-cells. We show that mice lacking both DLL1 and DLL4 in adult β-cells display improved glucose tolerance, increased glucose-stimulated insulin secretion and hyperglucagonemia. In contrast, overexpression of the intracellular domain of DLL1 in adult murine pancreatic β-cells results in impaired glucose tolerance and reduced insulin secretion, both *in vitro* and *in vivo*. These results suggest that NOTCH ligands play specific roles in the adult pancreas and highlight a novel function of the Delta-Notch pathway in β-cell insulin secretion.

KEYWORDS

Delta-Notch, diabetes, insulin secretion, pancreatic β-cells

ABBREVIATIONS

Cdkn1a, 1c	Cyclin Dependent Kinase Inhibitor 1a, -1c
D/N	Delta-Notch
DICD	Delta intracellular domain
DLL1, -3, -4	Delta-like 1, -3, -4

EPAC2	Exchange protein directly activated by cAMP 2
GSIS	Glucose-stimulated insulin secretion
Jag1, -2	Jagged1, -2
Pdx1	Pancreatic and duodenal homeobox 1

Diabetes mellitus is a major metabolic disease with over 400 million people diagnosed and a large number of undiagnosed adults (1). Genome-wide association studies (GWAS) have implicated a large number of genes in the pathology of this disorder (2). Among these, the Delta/Notch (D/N) pathway components *Dll4* and *Notch2* were found to be associated with type-2 diabetes (3), sparking investigation into their roles in glucose metabolism. The highly conserved D/N signaling pathway is crucial for embryonic development in a wide range of different tissues (4). Although Notch activity is required during pancreatic development (5), some D/N components have also been reported to be active during adulthood. D/N signaling mediates cell-cycle regulation via transmembrane-bound ligands (DLL1, -3, -4/JAGGED1, -2) and receptors (NOTCH1-4). Studies have shown that DLL1 and DLL4 regulate tissue renewal and maintain intestinal progenitor cells (6). Furthermore, NOTCH/NEUROG3 signaling is active in adult rodent and human pancreatic islets (7). Two recent studies gave new insights into the regulation of β-cell function by NOTCH1 and DLL4 in adult mouse islets (8,9). Whereas NOTCH1 is reported to regulate β-cell maturation and proliferation (8), DLL4 is associated with regulation of islet function (9). To date, however, no comprehensive analysis of D/N pathway components has been performed in the adult pancreas.

Ligand binding to Notch receptors leads to proteolytic cleavages that in turn release the Notch-intracellular domain (NICD), which enters the nucleus and acts with cofactors as a

transcriptional regulator (10,11). Interestingly, the ligands also undergo proteolytic cleavage and release their intracellular domains, which can also enter the nucleus (12,13). However, their precise function is poorly understood (14,15). Moreover, the location and possible function of other D/N pathway components in the adult pancreas has yet to be determined. Considering that dysfunctional pancreatic β-cells are a major characteristic of type-2 diabetes (16), detailed studies of the D/N signaling pathway are required.

Here, we provide a broad expression analysis of selected D/N-pathway components in the mouse adult pancreas and report the presence of cell-type specific protein expression. Furthermore, we show that ligands DLL1 and DLL4 are active and play a role in β-cell insulin secretion by utilizing conditional β-cell-specific mouse models. Finally, we report the presence of the DLL1 intracellular domain (DICD) in adult β-cells and describe a possible function.

Research Design and Methods

Generation of transgenic mice. Mice carrying floxed alleles for both *Dll1* (17) and *Dll4* (18) (background Sv/129.C57BL/6 x C57BL/6J) were intercrossed with Pdx1-Cre^{ERT} (19) (C3HeB/FeJ) mice. *Cre*$^{+}$ heterozygous F1 offspring were intercrossed to acquire homozygous animals for *Dll1*, *Dll4* or both in F2. Homozygous mice with the same genetic background (Dll1$^{+/+}$Dll4$^{+/+}$, Dll1$^{lox/lox}$ Dll4$^{+/+}$, Dll1$^{+/+}$ Dll4$^{lox/lox}$ or Dll1$^{lox/lox}$Dll4$^{lox/lox}$) were used to create β-cell-specific homozygous lines lacking either *Dll1* (β-DLL1), *Dll4* (β-DLL4) or both simultaneously (β-D1D4). *Cre*$^{+}$ wild-type littermates were used as controls.

To generate a mouse model with overexpression of the DICD, we used gene targeting into the endogenous *Rosa26* locus by recombinase mediated cassette exchange (RMCE) (20). The cDNA sequence of DICD and the coding sequence of the fluorescent reporter IRES-VENUS cassette were cloned independently from each other into two TOPO TA Vectors (pENTRY

Clones). Subsequently, DICD and the reporter cassette were joined via homologue end-joining into a target vector (pEx-CAG-ROSA26), thus generating the pRMCE-DICD-IRES-VENUS donor vector (ESM Fig. 1A). To enable RMCE *in vivo*, the ΦC31/attP integrase-mediated recombination approach (21) was used in IDG3.2 ROSA26 acceptor embryonic stem cells (ES), which have a mixed C57BL6/J-129S6/SvEvTac genetic background (22). To avoid influence of the neomycin resistance cassette on genes near the target locus *Rosa26*, the pgk promoter and the neo-bpA cassette were removed by flippase-mediated removal. Successfully recombined ES cells were selected and used for blastocyst injection. Chimeric mice were mated with C57BL/6J wild-type mice to obtain germline transmission. The new mouse line was named Rosa26-DICD and outcrossed to C3HFeB/J wild-type mice for 5 generations.

The expression of the DICD-IRES-VENUS construct was driven by the *Cre*-mediated excision of the floxed puro-polyA stop cassette (ESM Fig. 1B). To specifically induce DICD expression in adult β-cells, Rosa26-DICD mice were intercrossed with Pdx1-Cre^{ERT} mice (19) and maintained on a C3HeB/FeJ background.

For all models, *Cre*-dependent recombination was activated in weaned offspring by feeding Tamoxifen®-containing chow (Genobius, 400mg/kg) for 4 weeks. Genotyping was done by PCR with specific primers, as listed in ESM Table 1. All experimental procedures were performed in accordance with German and European Union guidelines. All mice were housed in specific pathogen-free conditions with a 12-hour light/dark cycle and free access to food (standard chow diet, Altromin, 1328 – Hybridpellet) and water.

Tissue preparation and immunohistochemistry. Mice were sacrificed by cervical dislocation and pancreata were excised, fixed in 4% PFA-PBS for 20 minutes and then washed in PBS for 5 minutes followed by serial incubations in 9% and 15% sucrose solutions

for 1 hour each and overnight in 30% solution. Thereafter, pancreatic tissue was embedded in O.C.T. solution (Thermo Fisher Scientific) and frozen. 9-µm sections were cut using a Leica CM1850 Cryostat (Leica Microsystems) and 3 sections were placed each on a SuperFrost® Plus slide (Menzel-Gläser), maintaining >100 µm of distance between each slide. All antibodies used are described in ESM Tables 2 and 3, respectively. Sections were blocked with 5% BSA in PBST and subsequently incubated with appropriate primary antibodies overnight at 4°C. After washing, slides were incubated in suitable secondary antibodies at room temperature for 90 minutes. Finally, sections were washed and covered with Vectashield® mounting medium (Vector Laboratories). Whole-slide images were acquired using a Nanozoomer (Hamamatsu) and analyzed using NDP.view 2 software (Hamamatsu). Cell counter application on ImageJ software was used for counting and quantification of insulin, glucagon, Ki-67 and MAFB positive cells. A minimum of 120 islets or 3000 cells were counted per genotype. Final images were acquired using a Leica TCS SP5 confocal microscope.

Intraperitoneal glucose tolerance test (ipGTT). Mice were fasted overnight for 16 hours. Weight and basal blood levels were measured before an intraperitoneal administration of 2g/kg glucose (Braun). Blood glucose levels were measured at 5, 15, 30, 60 and 120 minutes post glucose administration and plasma was collected at 0, 15 and 30 minutes.

***In vitro* stimulatory studies and immunocytochemistry.** Islets were isolated from mice and maintained as described previously (23). Isolated islets were incubated with 1.5 mM glucose in Krebs-Ringer buffer for 2 hours. Next, islets (10/mouse/experiment) were stimulated for 2 hours at 37°C with different glucose concentrations along with 2.5 µM Forskolin (Sigma-Aldrich), 10 µM Norepinephrine (Sigma-Aldrich), 10 µM ESI-09 (Biozol), 30 mM KCl (Sigma-Aldrich) and 100 nM Exendin-4 (Sigma-Aldrich) in combination with 16.7 mM glucose. To assess the whole-islet protein content, unstimulated islets (10/mouse) were taken

and dissolved in acid ethanol. For immunocytochemistry, islets were dispersed in 0.05% Trypsin-EDTA (Sigma-Aldrich) for 5 minutes and allowed to settle on slides coated with Cell Tak (Corning) in serum-free medium for one hour. Cells were then fixed in 4% PFA-PBS for 10 minutes at RT and permeabilized in 0.3% Triton-X-100 for 15 minutes. Next, cells were blocked in 10% horse serum and incubated with primary antibodies for 2 hours and with secondary antibodies for 45 minutes. Images were acquired using Axio-Imager M.2 microscope (Zeiss) and were analyzed (~3000 cells per mouse) with QuPath (24) software v 0.1.2.

RNA Isolation, cDNA synthesis and quantitative real time PCR. Islet RNA isolation was performed with the RNeasy® Plus Micro Kit (QIAGEN) according to the manufacturer's instructions. qRT-PCR was used for amplification of cDNA samples, using the LightCycler® 480 DNA SYBR Green I Master (Roche) with primers listed in ESM Table 1. Crossing point (Cp) values were obtained with the automatic Cp analysis of the LightCycler® 480 software (Roche) using the second derivative maximum method. All subsequent data analysis was performed in Microsoft Excel. The results were determined using the equations outlined in the geNorm® 3.5 user manual, which are mathematically identical to the 2-ΔΔCp method (25).

Hormone assays. Insulin and glucagon obtained from *in vitro* stimulatory studies and plasma samples were analyzed using Mercodia Mouse Insulin ELISA kit and Mouse Glucagon ELISA kit according to the manufacturer's instructions.

Statistics. Statistical analysis was achieved using GraphPad Prism software and applied using heteroscedastic two-tailed student *t* test, one-way or two-way ANOVA with Bonferroni *post hoc* test for multiple comparisons. A value of $p<0.05$ was considered significant. Unless stated otherwise, all results are described as mean±SD.

Data and Resource Availability. All data generated or analyzed during the current study are included in the published article and online supplementary data.

Results

Expression of Delta/Notch pathway components in the adult murine pancreas. To analyze the expression of Notch receptors and ligands in adult pancreatic islets, we employed qRT-PCR analysis in wild-type C3HeB/FeJ mice. We found that the *Notch1*, *Notch2* genes, Notch ligands genes *Jag2* and *Dll4* as well as Notch target genes *Hes1* and *Hes6* were strongly expressed and at comparable levels, followed by the Notch ligand genes *Jag1 and Dll1,* (Fig. 1A). Minimal expression was detected for *Notch3* and *Notch4*, as well as for the target genes *Hey1* and *Hey2* (Fig. 1A), indicating differential expression of D/N components in adult islets. To visualize and quantify the islet cell-type specific expression pattern, we used ligand- and receptor-specific antibodies along with markers for α-, β- and δ-cells, and performed co-immunostainings on pancreatic sections and on dispersed islet cell types. Whereas, NOTCH1 expression was found in most α-, β- and δ-cells, NOTCH2 and NOTCH4 showed limited expression, with a small population (8%) of δ-cells expressing the former while that of (15%) β-cells expressing the latter (Fig. 1B, ESM Fig. 2). Interestingly, NOTCH3 expression was not detected in any islet cell type. (Fig. 1B, ESM Fig. 2). Similarly, JAGGED2 that although has high mRNA expression, was not detectable in the islets, while that of JAGGED1 was abundantly found in islets, with ~70% of α-cells expressing the ligand (Fig. 2, ESM Fig. 2). Conversely, DLL1 and DLL4 were found in most β-cells (~90%), while limited expression in α- and δ-cells (Fig. 2, ESM Fig. 2). These results demonstrate that D/N pathway components have a broad and heterogeneous expression pattern in adult mouse

islets, such as DLL1 and 4 expression in β-cells, strongly indicating functional relevance in a cell-type specific manner.

***Dll1* and *Dll4* are essential for normal glucose homeostasis**. Since in the adult mouse pancreas DLL1 and DLL4 are predominantly expressed in β-cells, we hypothesized that active Notch signaling either maintains β-cell homeostasis or is important for β-cell function. To test this idea, we generated different β-cell-specific homozygous knockout models for *Dll1*, *Dll4* and both genes simultaneously (see ESM Fig. 3A,B for breeding schemes). Since female mice are often protected from a diabetic phenotype (26) and for better comparison with other studies (8,9), only male mice were used in this study. After tamoxifen treatment, *Cre* expression was found specifically in islets (ESM Fig.3C) along with substantial decrease in *Dll1* and *Dll4* mRNA (ESM Fig. 3D), as well as a comparable decrease in protein expression (ESM Fig. 3E). The three mutant mouse lines (β-DLL1, β-DLL4 and β-D1D4, respectively) and control mice were investigated for body weight and blood glucose levels in an *ad libitum* fed state. β-DLL1 mice showed significantly increased blood glucose levels as compared to control mice (Fig. 3B). Body weight and blood glucose levels were not altered in β-DLL4 mice (Fig. 3A,B). However, knocking out both ligands in β-D1D4 mice resulted in significantly reduced blood glucose levels but unchanged body weight as compared to controls (Fig. 3B).

Due to differences in blood glucose levels between the groups, we wondered whether β-cell function was affected, especially in β-D1D4 mice. Therefore, we performed ipGTTs to investigate glucose disposal. Compared to controls, β-DLL1 mice showed a significant but only mild decrease in glucose tolerance accompanied with a significant reduction in insulin secretion (ESM Fig. 4A), whereas β-DLL4 mice displayed a significant albeit modest increase in glucose tolerance with no major changes in insulin secretion (ESM Fig. 4A). In β-D1D4 mice, we noticed a clear improvement in glucose tolerance (Fig. 3C) resulting in a

twofold increase in acute insulin response within the first 15 minutes (Fig. 3D,E). *Ad libitum* fed plasma insulin levels were unchanged in β-D1D4 mice compared to controls (Fig. 3F), as were the mRNA levels in isolated islets of both insulin gene isoforms (Fig. 3G), which was similar to the observations made for β-DLL1 and β-DLL4 islets (ESM Fig. 4B).

To confirm whether loss of DLL1 and DLL4 leads to abnormal insulin secretion, we analyzed β-D1D4 mice in a glucose-stimulated insulin secretion assay using isolated islets. Compared to controls, basal insulin secretion at low glucose concentration (2.8 mM) was not altered. However, at high glucose concentration (16.7 mM), we observed a 4-fold increase in insulin secretion (Fig. 3H). This was further potentiated upon stimulation with forskolin. By adding norepinephrine, which hyperpolarizes the cell and inhibits adenylyl cyclase (27), the increase in insulin secretion under high glucose conditions was normalized. Also the addition of ESI-0, which inhibits EPAC2, a downstream target of adenylyl cyclase (28), normalized insulin secretion under high glucose conditions (Fig. 3H). Therefore, the concomitant loss of DLL1 and DLL4 in adult pancreatic β-cells leads to enhanced glucose clearance due to an increase in insulin secretion.

Loss of *Dll1* and *Dll4* leads to overproduction of α-cells and hyperglucagonemia. To understand whether lack of Delta ligands leads to changes in the islet transcriptome, we carried out qRT-PCR to analyze gene expression of D/N pathway intermediates. Compared to control islets, the expression of Notch and Jagged components in β-DLL1 and β-DLL4 islets was largely unaffected with the exception of *Jag2* in islets of β-DLL1 mice (ESM Fig. 5A,B). Interestingly, β-D1D4 islets showed an upregulation of the α-cell-specific ligand *Jag1*, as well as a significant increase in the expression of *Notch1*, *2* and *4*, and the downstream target *Hes1* (ESM Fig. 5C). Next, immunohistochemical analysis of insulin and glucagon double-stained pancreas did not reveal major differences in glucagon- and insulin-positive cells in β-

DLL1 and β-DLL4 mutants compared to control mice (Fig. 4A-C, ESM Fig. 5D). However, significantly increased glucagon-positive staining was observed within β-D1D4 islets (Fig. 4D, ESM Fig. 5E). Consistent with this observation, no change was found in the insulin content of freshly isolated islets between the groups (Fig. 4E), whereas there was a significant increase in glucagon protein content in islets (Fig. 4F) and plasma (ESM Fig. 5F) from β-D1D4 mutants as compared to controls. To determine whether an increase in glucagon-positive α-cells accounted for hyperglucagonemia in β-D1D4 mice, we stained pancreatic sections with MAFB and glucagon as markers of mature α-cells. We observed a significant increase in both MAFB-positive cells and *Mafb* gene expression in β-D1D4 mice (Fig. 4G-I). Moreover, we found an increase in Ki-67 expression in glucagon-positive cells as well as increased glucagon gene expression in islets of β-D1D4 mice, indicating higher proliferation of α-cells in these mice compared to their wild-type littermates (Fig 4. J-L).

Next, we examined whether the increase in glucagon-positive α-cells in β-D1D4 mice was of β-cell origin, since the knockout of Delta ligand genes is specific to these cells due to CRE expression driven by the *Pdx1* promoter. Therefore, we stained pancreatic sections of mice for CRE and glucagon. As seen in Fig. 4M, we found CRE expression in the cytoplasm of β-cells in both groups before tamoxifen treatment (upper panel) and nuclear expression 2 weeks after treatment (lower panel) in glucagon-negative cells. Additionally, we did not find PDX1-positive cells expressing glucagon in β-D1D4 mice after tamoxifen treatment (ESM Fig. 5G). Taken together, the β-cell-specific deletion of both *Dll1* and *Dll4* in adult mice suggests autocrine effects causing increased glucose disposal due to increased insulin secretion and paracrine effects on neighboring non-β-cells.

The Delta-like 1 intracellular domain is required for normal glucose homeostasis

Previously, it was shown in *Drosophila* that Delta ligands lacking the intracellular domain were able to bind NOTCH but not to activate the pathway, strongly indicating an important functional role (29). Furthermore, *in vitro* studies showed that the DICD regulates nuclear signaling by binding to NICD (30), whereas in the cytoplasm it interacts with components of the TGFβ/activin cascade (31). To analyze the role of the DICD in the adult pancreas, we established a mouse model that conditionally overexpresses the DICD (referred to here as β-DICD) (ESM Fig. 1A and B). To search for possible influences of DICD overexpression on embryonic development, Rosa26-DICD mice were mated to EIIa-cre transgenic mice (32). In agreement with previous findings (14), analysis of homozygous F2 animals during embryonic development did not reveal any obvious phenotype (data not shown). Successful recombination and DICD overexpression after tamoxifen induction was confirmed on the DNA, mRNA and protein level (ESM Fig. 1C-E).

We analyzed male β-DICD mice *in vivo* and *in vitro* at 8 weeks of age. The *ad libitum* fed bodyweight of β-DICD mice was significantly reduced and blood glucose levels were slightly but significantly increased (Fig. 5A and B) compared to Cre^+ controls. During an ipGTT, β-DICD mice showed a significant delay in glucose disposal compared to controls (Fig. 5C). Accordingly, a significantly lower amount of secreted insulin was observed (Fig. 5D). However, β-DICD mice showed no significant change in *ad libitum* fed plasma insulin levels (Fig. 5E) or insulin gene expression in isolated islets (Fig. 5F). GSIS analysis in isolated islets under low-glucose conditions revealed no difference between β-DICD and control mice, and only a slight but non-significant reduction in insulin secretion under high-glucose conditions. However, additional stimulation with exendin-4 and forskolin revealed that significantly less insulin was secreted by β-DICD, again hinting at a possible connection of DLL1 with adenylyl cyclase (Fig. 5G).

Reduced insulin secretion in β-DICD mice is independent of islet architecture

Next, we wondered whether overexpression of DICD has any effect on islet morphology, β-cell proliferation and maturity. Comparison of islets from 8-week-old male β-DICD mice with *Cre*$^{+}$ controls revealed no obvious differences in their architecture and expression of insulin and glucagon (Fig. 6A). Accordingly, insulin and glucagon content per islet was comparable between the groups (Fig. 6B and C). Furthermore, no change in plasma glucagon was found in β-DICD islets (Fig. 6D). In agreement with this finding and the reported transcriptional activity of DICD (30), relative gene expression levels of *Notch1-4, Dll4* and *Jag1-2* were unaltered in β-DICD compared to control islets (Fig. 6E).

Previously, *Ctgf* (connective tissue growth factor), an intermediate of the TGF-β pathway, was found to be associated with DICD (33). Interestingly, although we found a strong downregulation of *Ctgf* in β-DICD islets, other genes with associated TGF-β signaling (*Smad2*, *Smad7* and *Mtor*) were not altered compared to control islets (Fig. 6F). In summary, the β-cell specific overexpression of DICD does not affect islet morphology, islet hormonal content and gene expression of D/N pathway intermediates, but results in a specific insulin secretion defect.

Discussion

In this study, we confirmed the presence of several mediators of the D/N pathway and several features of its components in adult pancreatic islets. Whereas NOTCH2 and 4 are expressed in some islet cells that in turn indicates heterogeneity in the expression of these proteins, NOTCH3 seems to be expressed in the vasculature, indicating a role in maintenance of blood vessel integrity (34). Consistent with a recent study (8), NOTCH1 was found within the whole adult pancreas, including the presence of activated NOTCH1 within islet nuclei. Moreover, JAGGED1 is specifically expressed in α-cells, indicating the presence of an active

NOTCH-JAGGED signaling pathway. Finally, DLL1 and DLL4 are highly expressed in β-cells, indicating divergence in the expression pattern of Notch ligands in the adult pancreas and therefore strongly suggesting a novel functional role. In light of these results, we employed β-cell specific knockouts of DLL1 and DLL4 to examine the potential roles of Delta ligands in the homeostasis of adult islets and provide further evidence of bi-directional D/N signaling by demonstrating importance of DICD in β-cell function.

A recent study demonstrated that loss of *Notch1* in adult β-cells protects mice from developing glucose intolerance as a consequence of diet-induced obesity (8). Therefore, loss of NOTCH1 signaling in adult mouse β-cells leads to a better metabolic profile (8), a feature similar to concomitant loss of *Dll1* and *Dll4* shown in the current study. However, β-DLL1 mice displayed mild hyperglycemia and impaired glucose tolerance without any observable changes in β- and α-cell mass, and although β-DLL4 mice displayed normoglycemia, *in vivo* glucose tolerance in β-DLL4 mice was mildly but significantly improved. This was accentuated by simultaneous loss of both Delta ligands, where a dramatic improvement in glucose tolerance was observed that mimicked loss of NOTCH1 in β-cells (8). The phenotypic discrepancy between β-DLL1 and β-DLL4 mice is rather puzzling but we speculate that the differences arise due to divergence in downstream targets upon Notch receptor activation by either DLL1 or DLL4, which are well documented across species and different organ systems (35-37). Moreover, NOTCH1 has been shown to have intrinsic selectivity for DLL4 over DLL1 *in vitro* (38). However, NOTCH1 activation by either of the Delta ligands is also organ and cell type specific (6,39), and in the case of murine β-cells, loss of NOTCH1 signaling phenotypically mimics loss of DLL4 somewhat, thereby presenting DLL4 as the major D/N player in the context of adult β-cell homeostasis.

Interestingly, a recent study utilized anti-DLL4 antibody administration in mice and reported an increase in insulin production by blocking the DLL4 protein, possibly as a consequence of increased β-cell proliferation (9). Moreover, upregulation of NOTCH1 in β-cells leads to increased proliferation of these cells (8). Therefore, it seems that the two scenarios, loss of Delta ligands and loss of Notch receptors, do not display entirely similar phenotypes. This indicates that despite loss of Delta ligands, Notch receptor signaling may still be activated. Billiard and colleagues (9) did not further investigate the state of Notch, but we observed an increase in transcripts of Notch receptors in β-D1D4 mice, including that of the downstream target *Hes1*. Hence, it is likely that Notch signaling is activated by other ligands from neighboring cells when expressions of Delta ligands are downregulated. Here, we showed that JAG1 is specifically expressed in α-cells. We speculate that JAG1 activates Notch signaling in islets of β-D1D4 mice. Indeed, we observed an increase in α-cell proliferation and glucagon levels, along with increased expression of the α-cell maturity marker *Mafb* and of *Jag1*. This, however, will require molecular investigation for further confirmation.

Interestingly, β-DLL1 mice*,* in which also the DICD is deleted, display mildly increased *ad libitum* fed blood glucose levels. However, overexpression of DICD in mice also led to higher blood glucose levels. This discrepancy is likely explained by an effect of the DICD on insulin secretion independently of the D/N pathway, whereas knocking down *Dll1* likely dampens paracrine signaling with regards to DLL1-NOTCH in the β-cells. Therefore, effects associated with overexpression of the DICD must arise from within the cell. In this regard, a study on DICD revealed an association with the TGFβ pathway and connective tissue growth factor *(Ctgf)* (33), which has been shown to be required for β-cell maturity and proliferation in islets (40,41). In fact, we observed a significant down regulation of *Ctgf* in β-DICD mice. However, the study by Riley et al. (41) was performed after partial β-cell destruction and

under non-stimulatory conditions, and no changes in maturity and proliferation of β-cells were observed.

Previously, studies have confirmed binding of DLL1 and DLL4 intracellular domains to PDZ domain-containing MAGUK proteins such as MAGI1 and 2 (12,42,43). Interestingly, both MAGI1 and 2 bind to RAPGEF2, a guanine nucleotide exchange factor for the small GTPase RAP1A (44,45). Furthermore, components of the GEF family are critical for K_{ATP}- and Ca^{2+} channel-dependent insulin secretion (46), and RAP1A interaction with EPAC2 (RAPGEF4) (47) is essential for first phase insulin secretion (48). Considering that EPAC2 is one of two pathways downstream of adenylyl cyclase (49,50), it is tempting to speculate that manipulation of DICD expression might have consequences for the availability of MAGI proteins to interact with RAPGEF2 and in turn affect its interaction with EPAC2/RAP1A-associated insulin secretion. Several lines of evidence are presented in support of this possibility. Firstly, although some downstream defects might be present since only a modest increase in insulin secretion was observed upon KCl stimulation, it is upon forskolin stimulation that revealed a lack of considerable potentiation in β-DICD. Secondly, a significant increase in insulin secretion was observed with forskolin in β-D1D4 islets. Finally, this significant increase in insulin secretion in β-D1D4 islets can be normalized by inhibiting adenylyl cyclase with norepinephrine and inhibiting EPAC2 by ESI-09. A graphical summary and schematic diagram of the proposed mechanism for DLL1/4-mediated influence on insulin secretion is given in Fig. 7E.

Conflicts of interest. No potential conflicts of interest relevant to this article were reported.

Funding. This work has been funded by the German Federal Ministry of Education and Research (BMBF) to the German Center for Diabetes Research (DZD e.V.).

Acknowledgements. We thank Prof. Freddy Radtke (École Polytechnique Fédérale de Lausanne (EPFL), Lausanne, Switzerland) for providing us with floxed *Dll1* and *Dll4* Sv/129.C57BL/6 x C57BL/6J mice. Pdx1-Cre^{ERT} mice were a kind gift of Prof. Maureen Gannon (Vanderbilt University Medical Center, Nashville, TN, USA). DICD rat monoclonal antibody was provided by Dr. Elisabeth Kremmer (Monoclonal antibody core facility, Helmholtz Zentrum München, Neuherberg, Germany). The authors also thank Anna-Lena Amend, Sandra Hoffman, Andreas Mayer and Michael Schulz (Institute of Experimental Genetics and German Mouse Clinic, Helmholtz Zentrum München, Neuherberg, Germany) for providing excellent technical assistance.

MR designed the study, carried out the research, collected and analyzed data and wrote the manuscript. NFC performed experiments, analyzed and interpreted the results and wrote the manuscript. DG generated the β-DICD mouse line and ASM carried out experiments. HL, GP and MHdA conceived and designed the study, contributed to the interpretation of results and critically reviewed the manuscript. GP and MHdA are the guarantors of this work and, as such, had full access to all the data in the study and take responsibility for the integrity of the data and the accuracy of the data analysis. All authors approved the final version of the manuscript.

Prior Presentation. Parts of this study were presented in poster form, entitled “Dll1 and Dll4-mediated Notch signaling in adult pancreatic beta cells is essential for the structural integrity of islets and maintenance of glucose homeostasis” at The Allied Genetics Conference 2016 (Orlando, Florida, USA) and EASD 2016 (Munich, Germany).

References

1. International Diabetes Federation. IDF Diabetes Atlas, 8th edn. Brussels, Belgium: International Diabetes Federation, 2017
2. Ashcroft FM, Rorsman P: Diabetes mellitus and the beta cell: the last ten years. Cell 2012;148:1160-1171
3. Morris AP, Voight BF, Teslovich TM, Ferreira T, Segre AV, Steinthorsdottir V, Strawbridge RJ, Khan H, Grallert H, Mahajan A, Prokopenko I, Kang HM, Dina C, Esko T, Fraser RM, Kanoni S, Kumar A, Lagou V, Langenberg C, Luan J, Lindgren CM, Muller-Nurasyid M, Pechlivanis S, Rayner NW, Scott LJ, Wiltshire S, Yengo L, Kinnunen L, Rossin EJ, Raychaudhuri S, Johnson AD, Dimas AS, Loos RJ, Vedantam S, Chen H, Florez JC, Fox C, Liu CT, Rybin D, Couper DJ, Kao WH, Li M, Cornelis MC, Kraft P, Sun Q, van Dam RM, Stringham HM, Chines PS, Fischer K, Fontanillas P, Holmen OL, Hunt SE, Jackson AU, Kong A, Lawrence R, Meyer J, Perry JR, Platou CG, Potter S, Rehnberg E, Robertson N, Sivapalaratnam S, Stancakova A, Stirrups K, Thorleifsson G, Tikkanen E, Wood AR, Almgren P, Atalay M, Benediktsson R, Bonnycastle LL, Burtt N, Carey J, Charpentier G, Crenshaw AT, Doney AS, Dorkhan M, Edkins S, Emilsson V, Eury E, Forsen T, Gertow K, Gigante B, Grant GB, Groves CJ, Guiducci C, Herder C, Hreidarsson AB, Hui J, James A, Jonsson A, Rathmann W, Klopp N, Kravic J, Krjutskov K, Langford C, Leander K, Lindholm E, Lobbens S, Mannisto S, Mirza G, Muhleisen TW, Musk B, Parkin M, Rallidis L, Saramies J, Sennblad B, Shah S, Sigurethsson G, Silveira A, Steinbach G, Thorand B, Trakalo J, Veglia F, Wennauer R, Winckler W, Zabaneh D, Campbell H, van Duijn C, Uitterlinden AG, Hofman A, Sijbrands E, Abecasis GR, Owen KR, Zeggini E, Trip MD, Forouhi NG, Syvanen AC, Eriksson JG, Peltonen L, Nothen MM, Balkau B, Palmer CN, Lyssenko V, Tuomi T, Isomaa B, Hunter DJ, Qi L, Wellcome Trust Case Control C, Meta-Analyses of G, Insulin-related traits Consortium I, Genetic Investigation of ATC, Asian Genetic Epidemiology Network-Type 2 Diabetes C, South Asian Type 2 Diabetes C, Shuldiner AR, Roden M, Barroso I, Wilsgaard T, Beilby J, Hovingh K, Price JF, Wilson JF, Rauramaa R, Lakka TA, Lind L, Dedoussis G, Njolstad I, Pedersen NL, Khaw KT, Wareham NJ, Keinanen-Kiukaanniemi SM, Saaristo TE, Korpi-Hyovalti E, Saltevo J, Laakso M, Kuusisto J, Metspalu A, Collins

FS, Mohlke KL, Bergman RN, Tuomilehto J, Boehm BO, Gieger C, Hveem K, Cauchi S, Froguel P, Baldassarre D, Tremoli E, Humphries SE, Saleheen D, Danesh J, Ingelsson E, Ripatti S, Salomaa V, Erbel R, Jockel KH, Moebus S, Peters A, Illig T, de Faire U, Hamsten A, Morris AD, Donnelly PJ, Frayling TM, Hattersley AT, Boerwinkle E, Melander O, Kathiresan S, Nilsson PM, Deloukas P, Thorsteinsdottir U, Groop LC, Stefansson K, Hu F, Pankow JS, Dupuis J, Meigs JB, Altshuler D, Boehnke M, McCarthy MI, Replication DIG, Meta-analysis C: Large-scale association analysis provides insights into the genetic architecture and pathophysiology of type 2 diabetes. Nature genetics 2012;44:981-990

4. Lai EC: Notch signaling: control of cell communication and cell fate. Development (Cambridge, England) 2004;131:965-973

5. Apelqvist A, Li H, Sommer L, Beatus P, Anderson DJ, Honjo T, Hrabe de Angelis M, Lendahl U, Edlund H: Notch signalling controls pancreatic cell differentiation. Nature 1999;400:877-881

6. Pellegrinet L, Rodilla V, Liu Z, Chen S, Koch U, Espinosa L, Kaestner KH, Kopan R, Lewis J, Radtke F: Dll1- and dll4-mediated notch signaling are required for homeostasis of intestinal stem cells. Gastroenterology 2011;140:1230-1240 e1231-1237

7. Dror V, Nguyen V, Walia P, Kalynyak TB, Hill JA, Johnson JD: Notch signalling suppresses apoptosis in adult human and mouse pancreatic islet cells. Diabetologia 2007;50:2504-2515

8. Bartolome A, Zhu C, Sussel L, Pajvani UB: Notch signaling dynamically regulates adult beta cell proliferation and maturity. The Journal of clinical investigation 2019;129:268-280

9. Billiard F, Karaliota S, Wang B, Stellas D, Serafimidis I, Manousopoulou A, Koutmani Y, Ninou E, Golubov J, DaNave A, Tsakanikas P, Xin Y, Zhang W, Sleeman M, Yancopoulos GD, Murphy AJ, Garbis SD, Karalis K, Skokos D: Delta-like Ligand-4-Notch Signaling Inhibition Regulates Pancreatic Islet Function and Insulin Secretion. Cell reports 2018;22:895-904

10. Ehebauer M, Hayward P, Martinez-Arias A: Notch Signaling Pathway. Science's STKE 2006;2006:cm7-cm7

11. Bray SJ: Notch signalling: a simple pathway becomes complex. Nature reviews Molecular cell biology 2006;7:678-689

12. Six EM, Ndiaye D, Sauer G, Laabi Y, Athman R, Cumano A, Brou C, Israel A, Logeat F: The notch ligand Delta1 recruits Dlg1 at cell-cell contacts and regulates cell migration. The Journal of biological chemistry 2004;279:55818-55826
13. Dyczynska E, Sun D, Yi H, Sehara-Fujisawa A, Blobel CP, Zolkiewska A: Proteolytic processing of delta-like 1 by ADAM proteases. The Journal of biological chemistry 2007;282:436-444
14. Redeker C, Schuster-Gossler K, Kremmer E, Gossler A: Normal Development in Mice Over-Expressing the Intracellular Domain of DLL1 Argues against Reverse Signaling by DLL1 In Vivo. PloS one 2013;8:e79050
15. Mishra-Gorur K, Rand MD, Perez-Villamil B, Artavanis-Tsakonas S: Down-regulation of Delta by proteolytic processing. The Journal of cell biology 2002;159:313-324
16. Remedi MS, Emfinger C: Pancreatic β-cell identity in diabetes. Diabetes, Obesity and Metabolism 2016;18:110-116
17. Hozumi K, Negishi N, Suzuki D, Abe N, Sotomaru Y, Tamaoki N, Mailhos C, Ish-Horowicz D, Habu S, Owen MJ: Delta-like 1 is necessary for the generation of marginal zone B cells but not T cells in vivo. Nature immunology 2004;5:638-644
18. Koch U, Fiorini E, Benedito R, Besseyrias V, Schuster-Gossler K, Pierres M, Manley NR, Duarte A, Macdonald HR, Radtke F: Delta-like 4 is the essential, nonredundant ligand for Notch1 during thymic T cell lineage commitment. The Journal of experimental medicine 2008;205:2515-2523
19. Zhang H, Fujitani Y, Wright CVE, Gannon M: Efficient recombination in pancreatic islets by a tamoxifen-inducible Cre-recombinase. genesis 2005;42:210-217
20. Nyabi O, Naessens M, Haigh K, Gembarska A, Goossens S, Maetens M, De Clercq S, Drogat B, Haenebalcke L, Bartunkova S, De Vos I, De Craene B, Karimi M, Berx G, Nagy A, Hilson P, Marine JC, Haigh JJ: Efficient mouse transgenesis using Gateway-compatible ROSA26 locus targeting vectors and F1 hybrid ES cells. Nucleic acids research 2009;37:e55
21. Belteki G, Gertsenstein M, Ow DW, Nagy A: Site-specific cassette exchange and germline transmission with mouse ES cells expressing phiC31 integrase. Nature biotechnology 2003;21:321-324

22. Chen CM, Krohn J, Bhattacharya S, Davies B: A comparison of exogenous promoter activity at the ROSA26 locus using a PhiiC31 integrase mediated cassette exchange approach in mouse ES cells. PloS one 2011;6:e23376
23. Li DS, Yuan YH, Tu HJ, Liang QL, Dai LJ: A protocol for islet isolation from mouse pancreas. Nature protocols 2009;4:1649-1652
24. Bankhead P, Loughrey MB, Fernandez JA, Dombrowski Y, McArt DG, Dunne PD, McQuaid S, Gray RT, Murray LJ, Coleman HG, James JA, Salto-Tellez M, Hamilton PW: QuPath: Open source software for digital pathology image analysis. Scientific reports 2017;7:16878
25. Livak KJ, Schmittgen TD: Analysis of relative gene expression data using real-time quantitative PCR and the 2(-Delta Delta C(T)) Method. Methods 2001;25:402-408
26. Tiano JP, Mauvais-Jarvis F: Importance of oestrogen receptors to preserve functional beta-cell mass in diabetes. Nature reviews Endocrinology 2012;8:342-351
27. Straub SG, Sharp GW: Evolving insights regarding mechanisms for the inhibition of insulin release by norepinephrine and heterotrimeric G proteins. American journal of physiology Cell physiology 2012;302:C1687-1698
28. Almahariq M, Tsalkova T, Mei FC, Chen H, Zhou J, Sastry SK, Schwede F, Cheng X: A Novel EPAC-Specific Inhibitor Suppresses Pancreatic Cancer Cell Migration and Invasion. Molecular Pharmacology 2013;83:122-128
29. Parks AL, Stout JR, Shepard SB, Klueg KM, Dos Santos AA, Parody TR, Vaskova M, Muskavitch MA: Structure-function analysis of delta trafficking, receptor binding and signaling in Drosophila. Genetics 2006;174:1947-1961
30. Jung J, Mo JS, Kim MY, Ann EJ, Yoon JH, Park HS: Regulation of Notch1 signaling by Delta-like ligand 1 intracellular domain through physical interaction. Molecules and cells 2011;32:161-165
31. Hiratochi M, Nagase H, Kuramochi Y, Koh CS, Ohkawara T, Nakayama K: The Delta intracellular domain mediates TGF-beta/Activin signaling through binding to Smads and has an important bi-directional function in the Notch-Delta signaling pathway. Nucleic acids research 2007;35:912-922
32. Lakso M, Pichel JG, Gorman JR, Sauer B, Okamoto Y, Lee E, Alt FW, Westphal H: Efficient in vivo manipulation of mouse genomic sequences at the zygote stage.

Proceedings of the National Academy of Sciences of the United States of America 1996;93:5860-5865
33. Bordonaro M, Tewari S, Atamna W, Lazarova DL: The Notch ligand Delta-like 1 integrates inputs from TGFbeta/Activin and Wnt pathways. Experimental cell research 2011;317:1368-1381
34. Henshall TL, Keller A, He L, Johansson BR, Wallgard E, Raschperger E, Mae MA, Jin S, Betsholtz C, Lendahl U: Notch3 is necessary for blood vessel integrity in the central nervous system. Arteriosclerosis, thrombosis, and vascular biology 2015;35:409-420
35. Nandagopal N, Santat LA, LeBon L, Sprinzak D, Bronner ME, Elowitz MB: Dynamic Ligand Discrimination in the Notch Signaling Pathway. Cell 2018;172:869-880 e819
36. Mohtashami M, Shah DK, Nakase H, Kianizad K, Petrie HT, Zuniga-Pflucker JC: Direct comparison of Dll1- and Dll4-mediated Notch activation levels shows differential lymphomyeloid lineage commitment outcomes. Journal of immunology 2010;185:867-876
37. Preusse K, Tveriakhina L, Schuster-Gossler K, Gaspar C, Rosa AI, Henrique D, Gossler A, Stauber M: Context-Dependent Functional Divergence of the Notch Ligands DLL1 and DLL4 In Vivo. PLoS genetics 2015;11:e1005328
38. Andrawes MB, Xu X, Liu H, Ficarro SB, Marto JA, Aster JC, Blacklow SC: Intrinsic selectivity of Notch 1 for Delta-like 4 over Delta-like 1. The Journal of biological chemistry 2013;288:25477-25489
39. Tveriakhina L, Schuster-Gossler K, Jarrett SM, Andrawes MB, Rohrbach M, Blacklow SC, Gossler A: The ectodomains determine ligand function in vivo and selectivity of DLL1 and DLL4 toward NOTCH1 and NOTCH2 in vitro. eLife 2018;7
40. Crawford LA, Guney MA, Oh YA, Deyoung RA, Valenzuela DM, Murphy AJ, Yancopoulos GD, Lyons KM, Brigstock DR, Economides A, Gannon M: Connective tissue growth factor (CTGF) inactivation leads to defects in islet cell lineage allocation and beta-cell proliferation during embryogenesis. Molecular endocrinology (Baltimore, Md) 2009;23:324-336
41. Riley KG, Pasek RC, Maulis MF, Peek J, Thorel F, Brigstock DR, Herrera PL, Gannon M: Connective tissue growth factor modulates adult beta-cell maturity and proliferation to promote beta-cell regeneration in mice. Diabetes 2015;64:1284-1298

42. Pfister S, Przemeck GK, Gerber JK, Beckers J, Adamski J, Hrabe de Angelis M: Interaction of the MAGUK family member Acvrinp1 and the cytoplasmic domain of the Notch ligand Delta1. Journal of molecular biology 2003;333:229-235
43. Wright GJ, Leslie JD, Ariza-McNaughton L, Lewis J: Delta proteins and MAGI proteins: an interaction of Notch ligands with intracellular scaffolding molecules and its significance for zebrafish development. Development 2004;131:5659-5669
44. Sakurai A, Fukuhara S, Yamagishi A, Sako K, Kamioka Y, Masuda M, Nakaoka Y, Mochizuki N: MAGI-1 Is Required for Rap1 Activation upon Cell-Cell Contact and for Enhancement of Vascular Endothelial Cadherin-mediated Cell Adhesion. Molecular Biology of the Cell 2006;17:966-976
45. Ohtsuka T, Hata Y, Ide N, Yasuda T, Inoue E, Inoue T, Mizoguchi A, Takai Y: nRap GEP: a novel neural GDP/GTP exchange protein for rap1 small G protein that interacts with synaptic scaffolding molecule (S-SCAM). Biochemical and biophysical research communications 1999;265:38-44
46. Shibasaki T, Sunaga Y, Seino S: Integration of ATP, cAMP, and Ca2+Signals in Insulin Granule Exocytosis. Diabetes 2004;53:S59-S62
47. Liao Y, Kariya K, Hu CD, Shibatohge M, Goshima M, Okada T, Watari Y, Gao X, Jin TG, Yamawaki-Kataoka Y, Kataoka T: RA-GEF, a novel Rap1A guanine nucleotide exchange factor containing a Ras/Rap1A-associating domain, is conserved between nematode and humans. The Journal of biological chemistry 1999;274:37815-37820
48. Shibasaki T, Takahashi H, Miki T, Sunaga Y, Matsumura K, Yamanaka M, Zhang C, Tamamoto A, Satoh T, Miyazaki J, Seino S: Essential role of Epac2/Rap1 signaling in regulation of insulin granule dynamics by cAMP. Proceedings of the National Academy of Sciences of the United States of America 2007;104:19333-19338
49. Seino S, Shibasaki T: PKA-Dependent and PKA-Independent Pathways for cAMP-Regulated Exocytosis. Physiological reviews 2005;85:1303-1342
50. Rutter Guy A, Pullen Timothy J, Hodson David J, Martinez-Sanchez A: Pancreatic β-cell identity, glucose sensing and the control of insulin secretion. Biochemical Journal 2015;466:203-218

Figure Legends

Fig. 1: Expression of Notch receptors in the adult pancreas. (**A**) qRT-PCR analysis of D/N components in isolated islets from 8-week-old male C3HeB/FeJ mice normalized to the housekeeping genes *Sdha and Ubc* ; n=5 (*Notch2* n=4). Data are shown as mean±SD. (**B**) Co-immunostaining of Notch receptors NOTCH1, NOTCH2, NOTCH3 and NOTCH4 with β- (insulin), α- (glucagon) and δ-cell (somatostatin) markers on pancreatic sections from 13-week-old male C3HeB/FeJ mice; n=3. Nuclei were counterstained with DAPI (blue). The scale bar represents 20 μm.

Fig. 2: Expression of Notch ligands in the adult pancreas. Co-immunostaining of DLL1, DLL4, JAGGED1 and JAGGED2 with β- (insulin), α- (glucagon) and δ-cell (somatostatin) markers on pancreatic sections from 13-week-old male C3HeB/FeJ; n=3. Nuclei were counterstained with DAPI (blue). The scale bar represents 20 μm.

Fig. 3: Glucose homeostasis in β-DLL1, β-DLL4 and β-D1D4 mice. (**A**) Average a*d libitum* fed body weight and (**B**) blood glucose levels; control n=8, β-DLL1 n=9, β-DLL4 n=7 and β-D1D4 n=10. (**C**) Intraperitoneal glucose-tolerance test (ipGTT); control n=16 and β-D1D4 n=18. (**D**) Plasma-insulin levels during ipGTT and (**E**) acute insulin response during ipGTT between t=0 min and t=15 min; control n=8 and β-D1D4 n=9. (**F**) Plasma insulin levels in *ad libitum* fed state; control n=10 and β-D1D4 n=9. (**G**) Relative gene expression levels of insulin gene isoforms in isolated islets; control n=10 and β-D1D4 n=6. Gene expressions were normalized to the housekeeping genes *Sdha* and *Ubc*. (**H**) Insulin secretion assay in isolated islets under several stimulants and 10 μM norepinephrine or 10 μM ESI-09; n=4. 8-10-week-old male mice were used in the study. Data for (C) and (D) are shown as mean ±SEM; all other data are shown as mean±SD. Differences were considered statistically

significant at $p<0.05$ using a two-way ANOVA with Bonferroni *post hoc* test and a two-tailed student *t* test (* $p<0.05$, ** $p<0.01$, *** $p<0.001$, **** $p<0.0001$).

Fig. 4: Islet integrity and hormone levels in β-DLL1, β-DLL4 and β-D1D4 mice. Immunostaining for insulin and glucagon in pancreatic sections of control (**A**), β-DLL1 (**B**), β-DLL4 (**C**) and β-D1D4 (**D**) mice; n=4. (**E**) Concentration of insulin and (**F**) glucagon in isolated islets from mutant and control mice; control n=18, β-DLL1 n=7, β-DLL4 and β-D1D4 n=8. (**G**) Immunostaining for glucagon and MAFB in pancreatic sections of β-D1D4 and control mice and (**H**) quantification of MAFB+ cells; 25-30 islets per genotype; n=4. (**I**) Relative gene expression of *Mafb*; control n=4 and β-D1D4 n=6. (**J**) Immunostaining for glucagon and Ki-67 positive islet cells and (**K**) quantification; n=4. (**L**) Relative gene expression levels of glucagon in isolated islets; control n=10 and β-D1D4 n=5. Gene expressions were normalized to the housekeeping genes *Sdha* and *Ubc*. (**M**) Immunostaining for glucagon and CRE before (week 0) and after (week 2) tamoxifen treatment; n=4-5. 8-week-old male mice were used in the study. Data are shown as mean±SD. Differences were considered statistically significant at $p<0.05$ using a one-way ANOVA with Bonferroni *post hoc* test and a two-tailed student *t* test (* $p<0.05$, ** $p<0.01$, *** $p<0.001$, **** $p<0.0001$).

Fig. 5: Glucose homeostasis in β-DICD mice. (**A**) Average *ad libitum* fed body weight; control n=10 and β-DICD n=9. (**B**) Blood glucose levels of mice; control n=8 and β-DICD n=10. (**C**) Measurement of blood glucose levels and (**D**) insulin during an intraperitoneal glucose tolerance test; control n=8 and β-DICD n=9. (**E**) Plasma insulin levels in *ad libitum* fed state; control n=12 and β-DICD n =11. (**F**) Relative gene expression levels of insulin in isolated islets; control n=11 and β-DICD n=9. Gene expressions were normalized to the housekeeping genes *Sdha* and *Ubc*. (**G**) Insulin secretion assay in isolated islets; control n=9

and β-DICD n=6. 8-week-old male mice were used in the study. Data for (C) and (D) are shown as mean±SEM; all other data are shown as mean±SD. Differences were considered statistically significant at $p<0.05$ using a two-way ANOVA with Bonferroni *post hoc* test and a two-tailed student *t* test (* $p<0.05$, ** $p<0.01$, *** $p<0.001$, **** $p<0.0001$).

Fig. 6: Islet integrity and hormone levels in β-DICD mice. (**A**) Immunostaining for insulin and glucagon in pancreatic sections; n=4-5. Scale bar represents 50 μm. (**B**) Concentration of insulin; n=7 and (**C**) glucagon in isolated islets; n=6. (**D**) Concentration of glucagon in plasma; n=10. Relative mRNA expression of (**E**) D/N components and (**F**) *Ctgf* as well as TGFβ pathway components in isolated islets; control n=5 and β-DICD n=4 (for *Dll4* n=3). Gene expressions were normalized to the housekeeping genes *Sdha* and *Ubc*. 8-week-old male mice were used in the study. Data are shown as mean±SD. Differences were considered statistically significant at $p<0.05$ using a two-tailed student *t* test (** $p<0.01$).

Fig 7: Graphical summary displaying (**A**) healthy pancreatic islet cell constituents, (**B**) cell-specific protein expression of D/N components within the wild-type islet, depicting α-cells (red), β-cells (green), δ-cells (yellow), non-endocrine cells (purple) and unlabeled cells (white) (**C**) a comparative illustration of a control vs. β-D1D4 islets and (**D**) a summary of the major phenotypic findings of the β-D1D4 and β-DICD mouse models. (**E**) Schematic diagram of the proposed DLL1/4-mediated influence on insulin secretion: RAP1A signaling is amplified by RAPGEF2, a factor that binds to MAGI proteins, which in turn can interact with the intracellular domains of DLL1 and DLL4. Differing expressions levels of these intracellular domains might have consequences for EPAC2/RAP1A-associated insulin secretion.

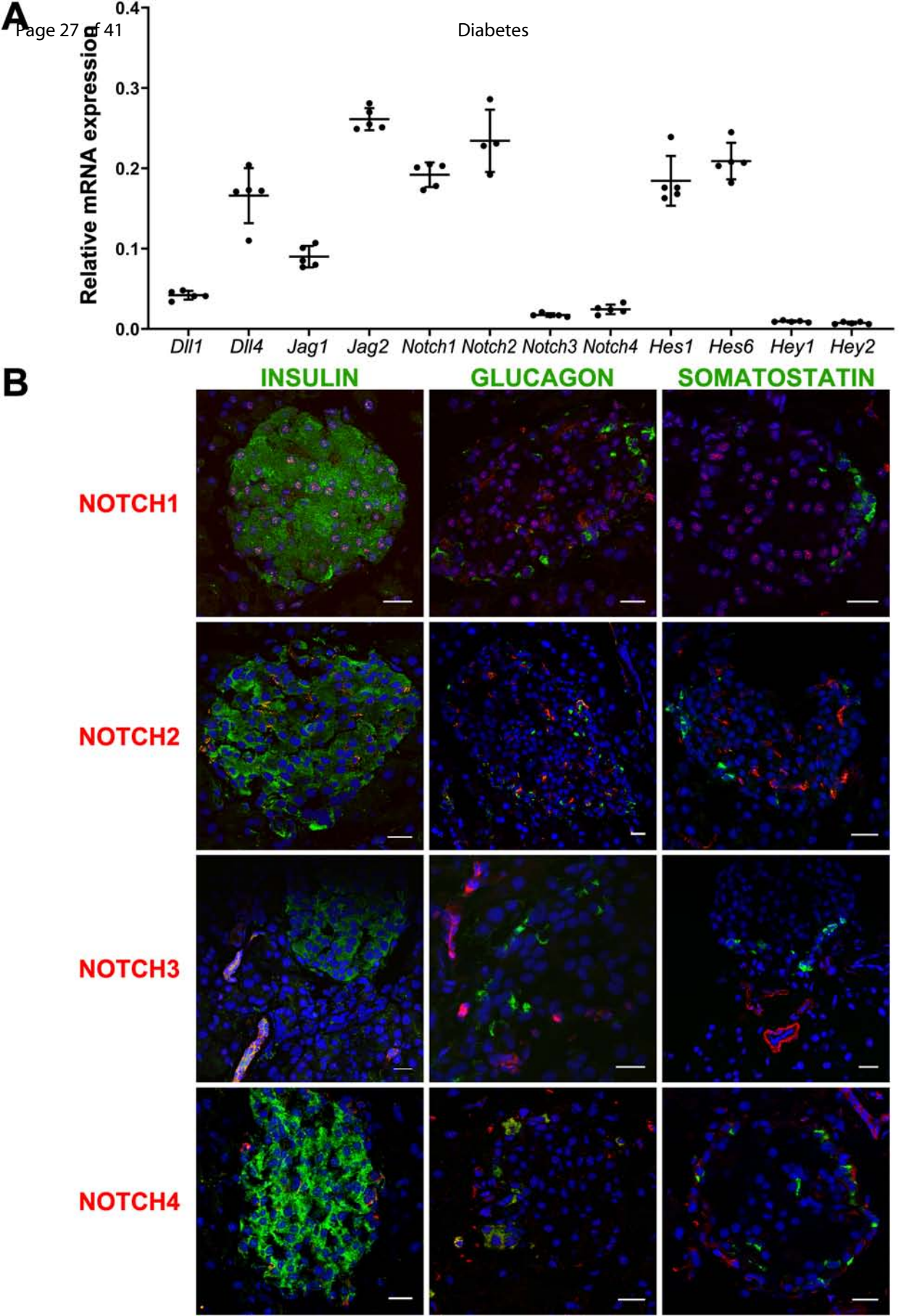
A
Relative mRNA expression
0.4
0.3
0.2
0.1
0.0
Dll1
Dll4
Jag1
Jag2
Notch1
Notch2
Notch3
Notch4
Hes1
Hes6
Hey1
Hey2
B
INSULIN
GLUCAGON
SOMATOSTATIN
NOTCH1
NOTCH2
NOTCH3
NOTCH4

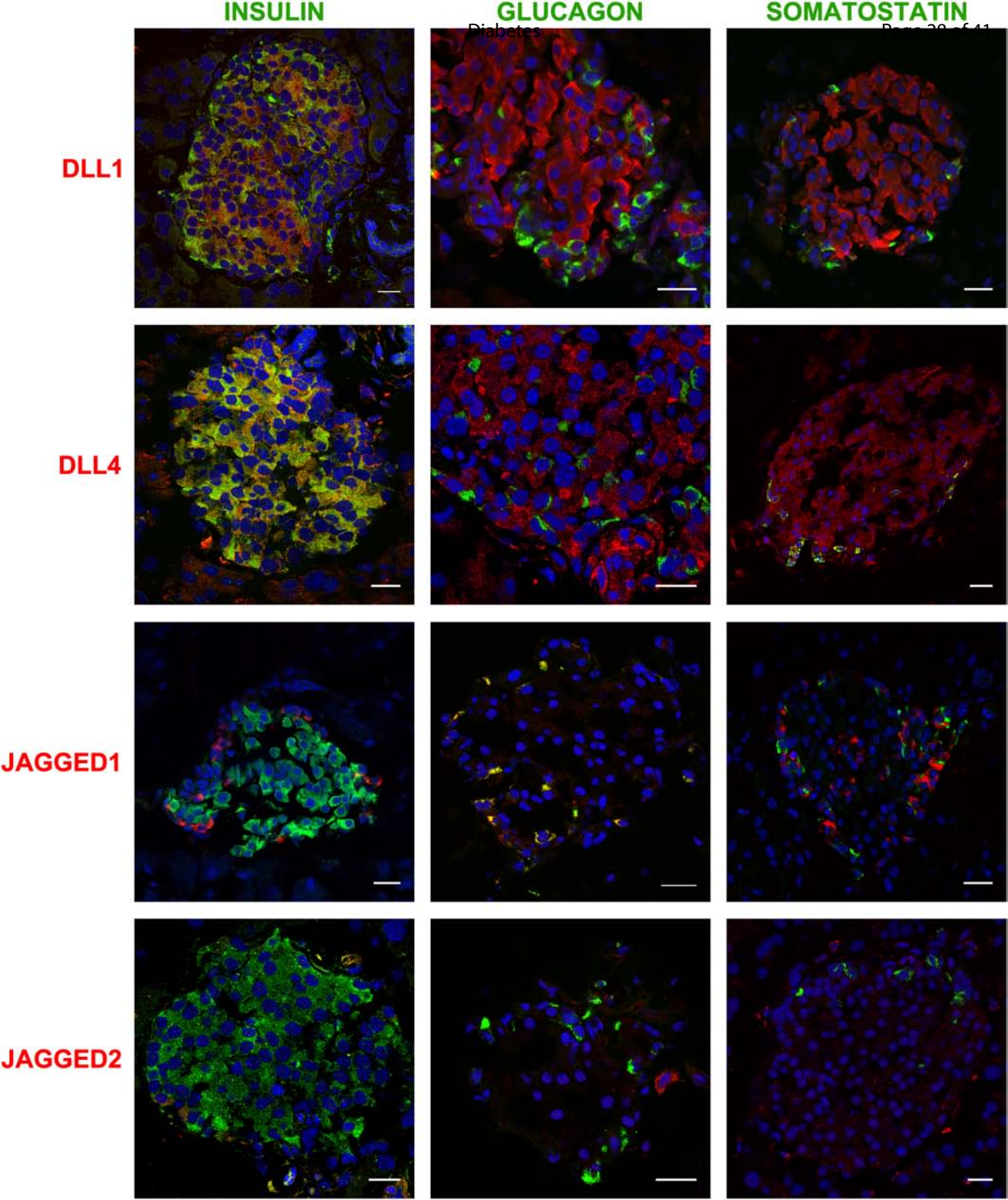
INSULIN
GLUCAGON
SOMATOSTATIN
DLL1
DLL4
JAGGED1
JAGGED2

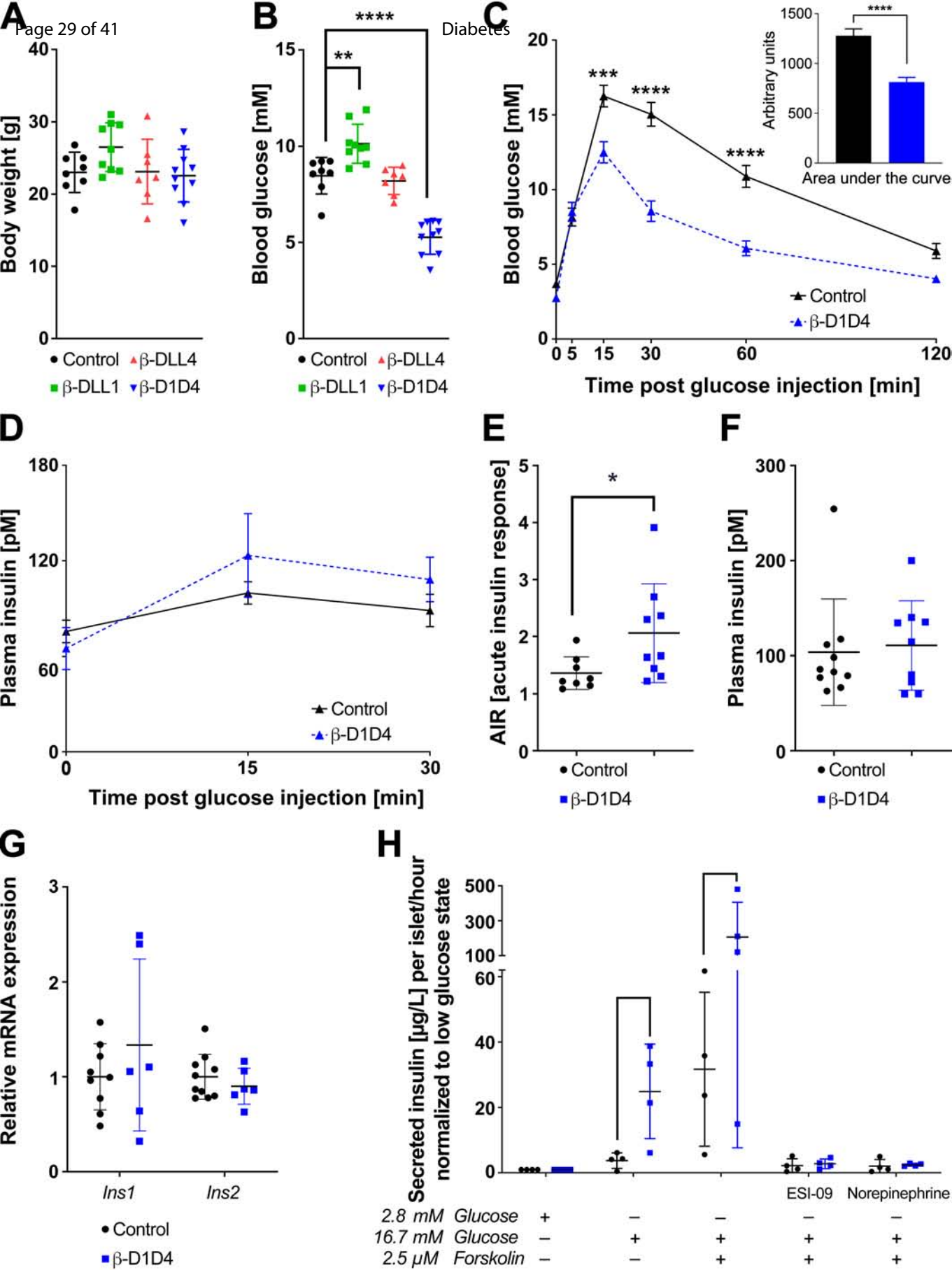
A
Body weight [g]
Control
β-DLL4
β-DLL1
β-D1D4
B
Blood glucose [mM]
**
****
C
Blood glucose [mM]
***
****
****
Control
β-D1D4
Time post glucose injection [min]
Arbitrary units
Area under the curve
D
Plasma insulin [pM]
Time post glucose injection [min]
E
AIR [acute insulin response]
*
F
Plasma insulin [pM]
G
Relative mRNA expression
Ins1
Ins2
H
Secreted insulin [µg/L] per islet/hour normalized to low glucose state
ESI-09
Norepinephrine
2.8 mM Glucose
16.7 mM Glucose
2.5 µM Forskolin

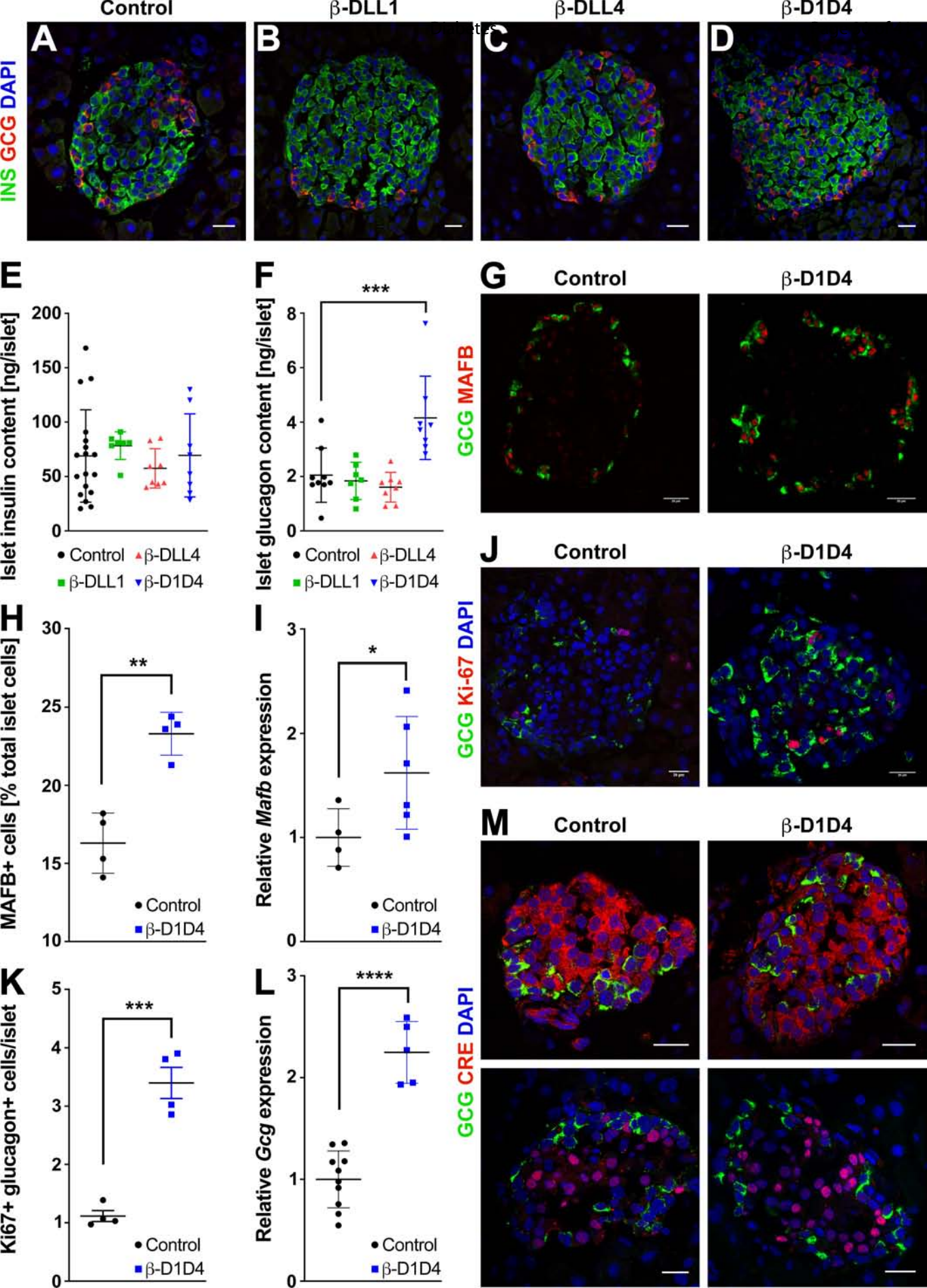
Control
β-DLL1
β-DLL4
β-D1D4
A
B
C
D
INS GCG DAPI
E
Islet insulin content [ng/islet]
200
150
100
50
0
Control
β-DLL4
β-DLL1
β-D1D4
F
Islet glucagon content [ng/islet]
***
8
6
4
2
0
Control
β-DLL4
β-DLL1
β-D1D4
G
Control
β-D1D4
GCG MAFB
J
Control
β-D1D4
GCG Ki-67 DAPI
H
MAFB+ cells [% total islet cells]
**
30
25
20
15
10
Control
β-D1D4
I
Relative Mafb expression
*
3
2
1
0
Control
β-D1D4
M
Control
β-D1D4
GCG CRE DAPI
K
Ki67+ glucagon+ cells/islet
***
5
4
3
2
1
0
Control
β-D1D4
L
Relative Gcg expression
****
3
2
1
0
Control
β-D1D4

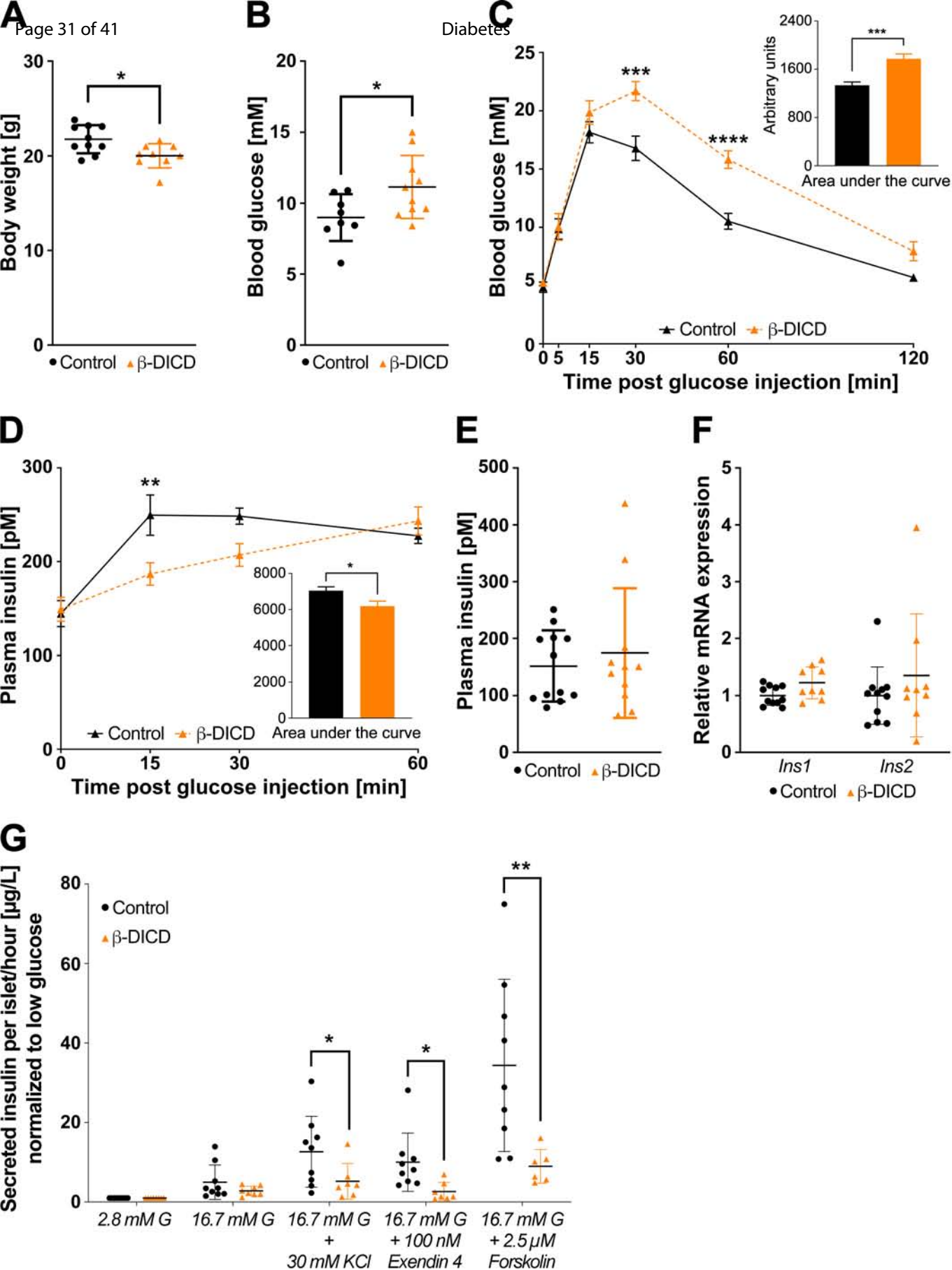
A
Body weight [g]
30
20
10
0
*
Control
β-DICD
B
Blood glucose [mM]
20
15
10
5
0
*
Control
β-DICD
C
Blood glucose [mM]
25
20
15
10
5
0
***
****
Control
β-DICD
0 5 15 30 60 120
Time post glucose injection [min]
Arbitrary units
2400
1600
800
0
***
Area under the curve
D
Plasma insulin [pM]
300
200
100
0
**
8000
6000
4000
2000
0
*
Control
β-DICD
Area under the curve
0 15 30 60
Time post glucose injection [min]
E
Plasma insulin [pM]
500
400
300
200
100
0
Control
β-DICD
F
Relative mRNA expression
5
4
3
2
1
0
Ins1
Ins2
Control
β-DICD
G
Secreted insulin per islet/hour [µg/L] normalized to low glucose
80
60
40
20
0
Control
β-DICD
*
*
**
2.8 mM G
16.7 mM G
16.7 mM G + 30 mM KCl
16.7 mM G + 100 nM Exendin 4
16.7 mM G + 2.5 µM Forskolin

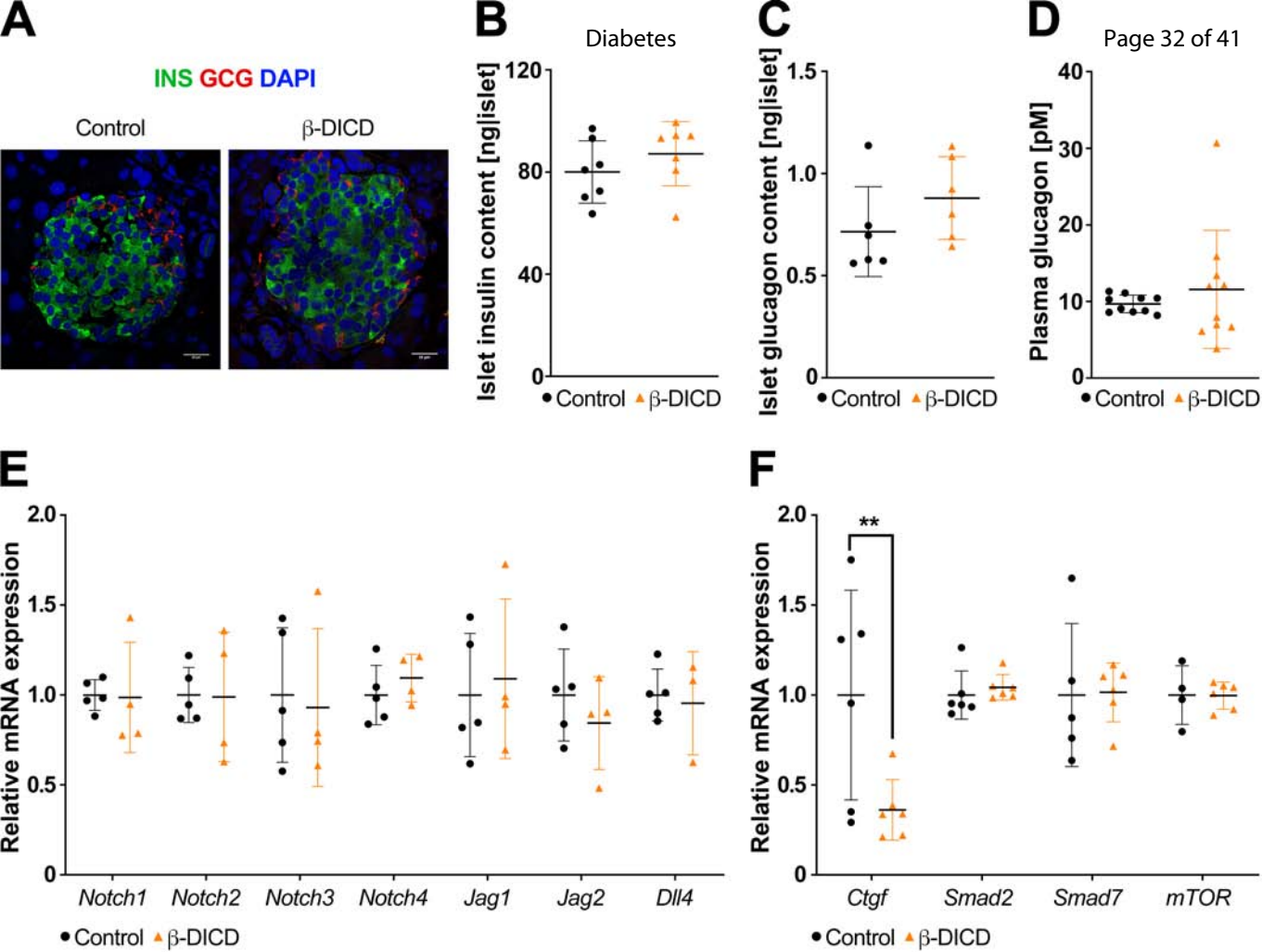
A
INS GCG DAPI
Control
β-DICD
B
Islet insulin content [ng|islet]
120
80
40
0
Control
β-DICD
C
Islet glucagon content [ng|islet]
1.5
1.0
0.5
0
Control
β-DICD
D
Plasma glucagon [pM]
40
30
20
10
0
Control
β-DICD
E
Relative mRNA expression
2.0
1.5
1.0
0.5
0
Notch1
Notch2
Notch3
Notch4
Jag1
Jag2
Dll4
Control
β-DICD
F
Relative mRNA expression
**
2.0
1.5
1.0
0.5
0
Ctgf
Smad2
Smad7
mTOR
Control
β-DICD

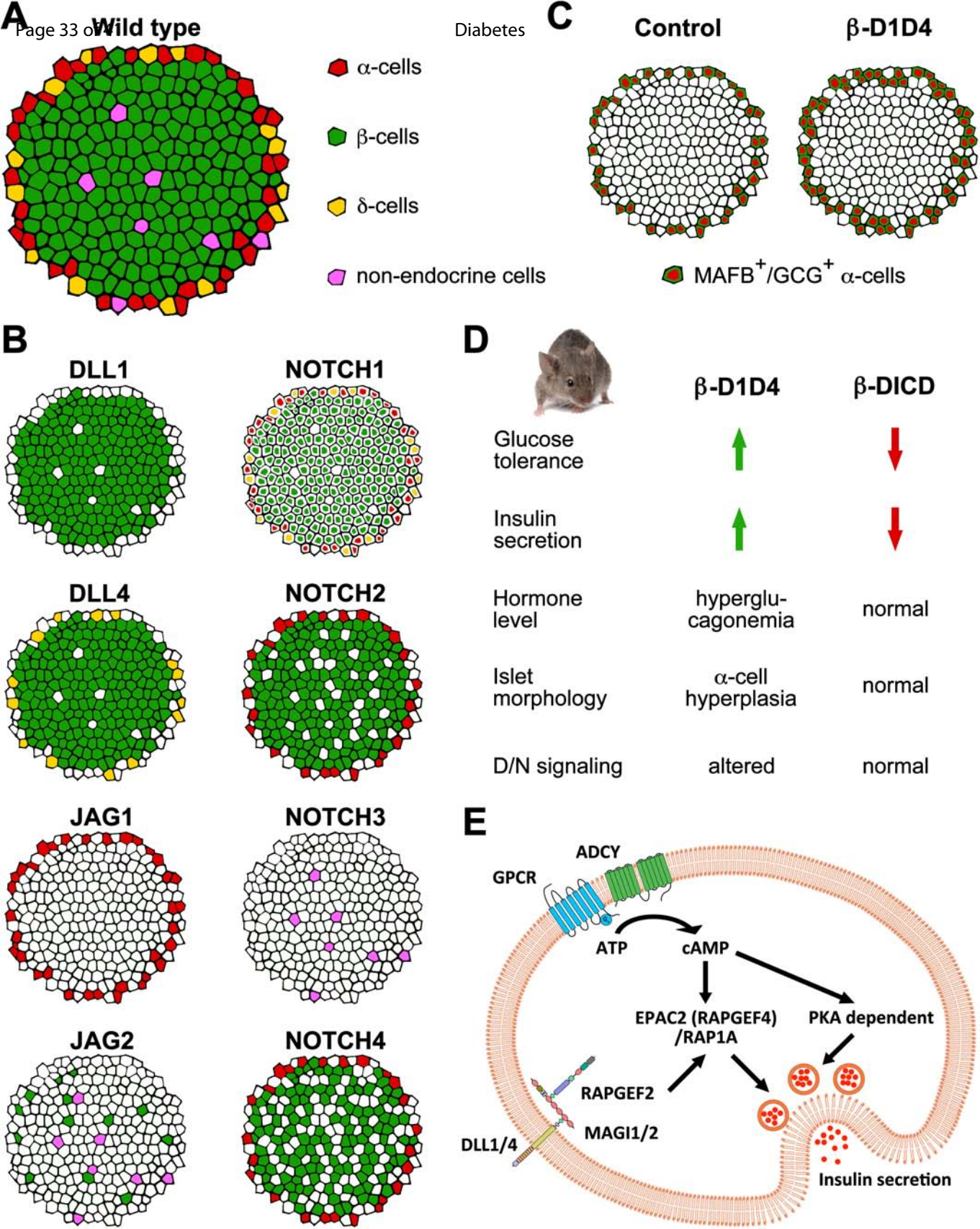
A
Wild type
α-cells
β-cells
δ-cells
non-endocrine cells
C
Control
β-D1D4
MAFB+/GCG+ α-cells
B
DLL1
NOTCH1
DLL4
NOTCH2
JAG1
NOTCH3
JAG2
NOTCH4
D
β-D1D4
β-DICD
Glucose tolerance
Insulin secretion
Hormone level
hyperglu-cagonemia
normal
Islet morphology
α-cell hyperplasia
normal
D/N signaling
altered
normal
E
ADCY
GPCR
ATP
cAMP
EPAC2 (RAPGEF4) /RAP1A
PKA dependent
RAPGEF2
MAGI1/2
DLL1/4
Insulin secretion

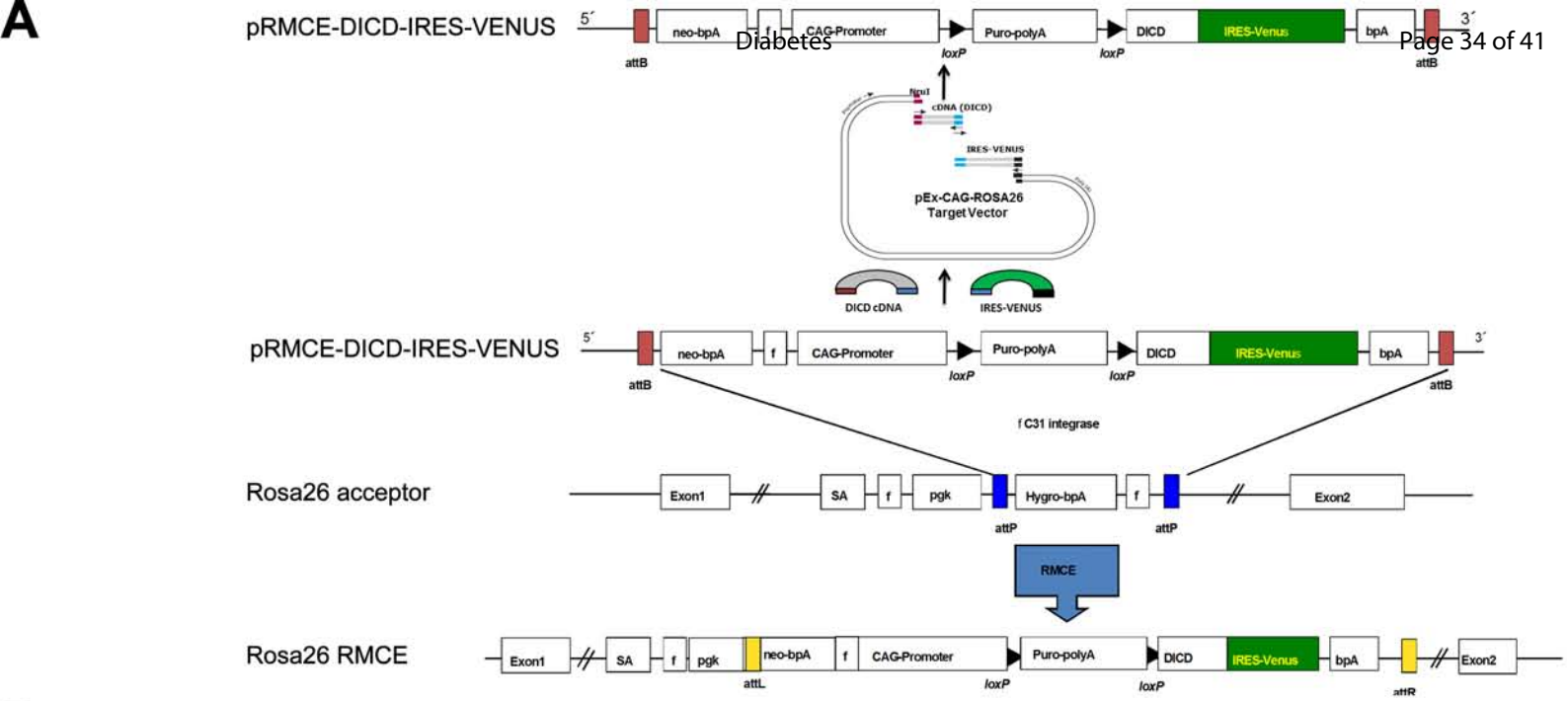

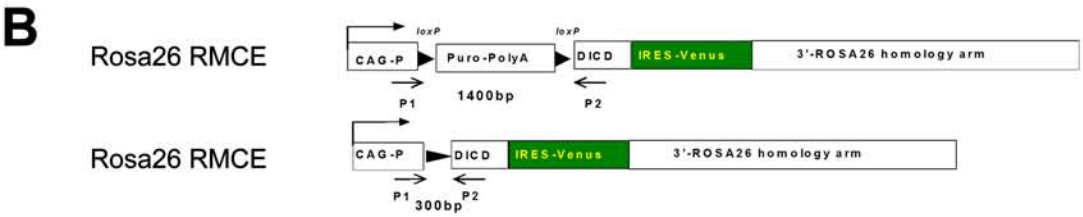

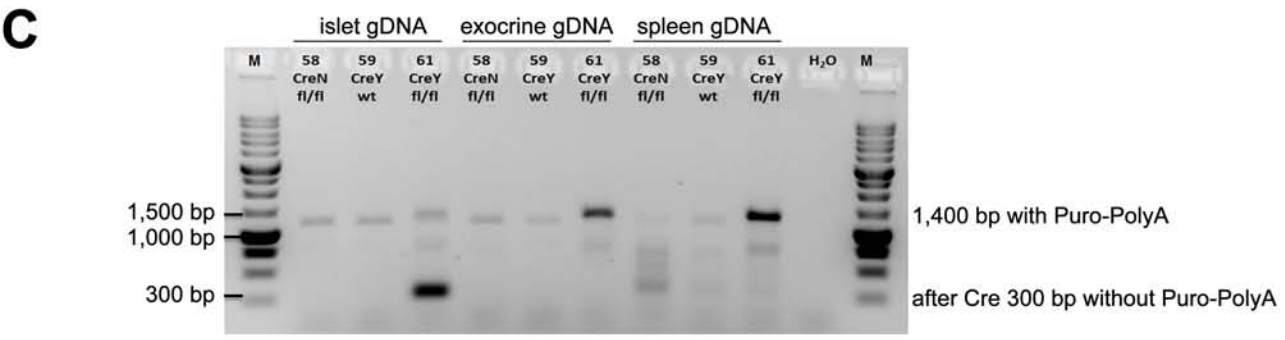

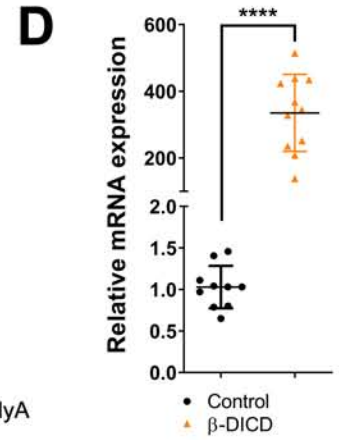

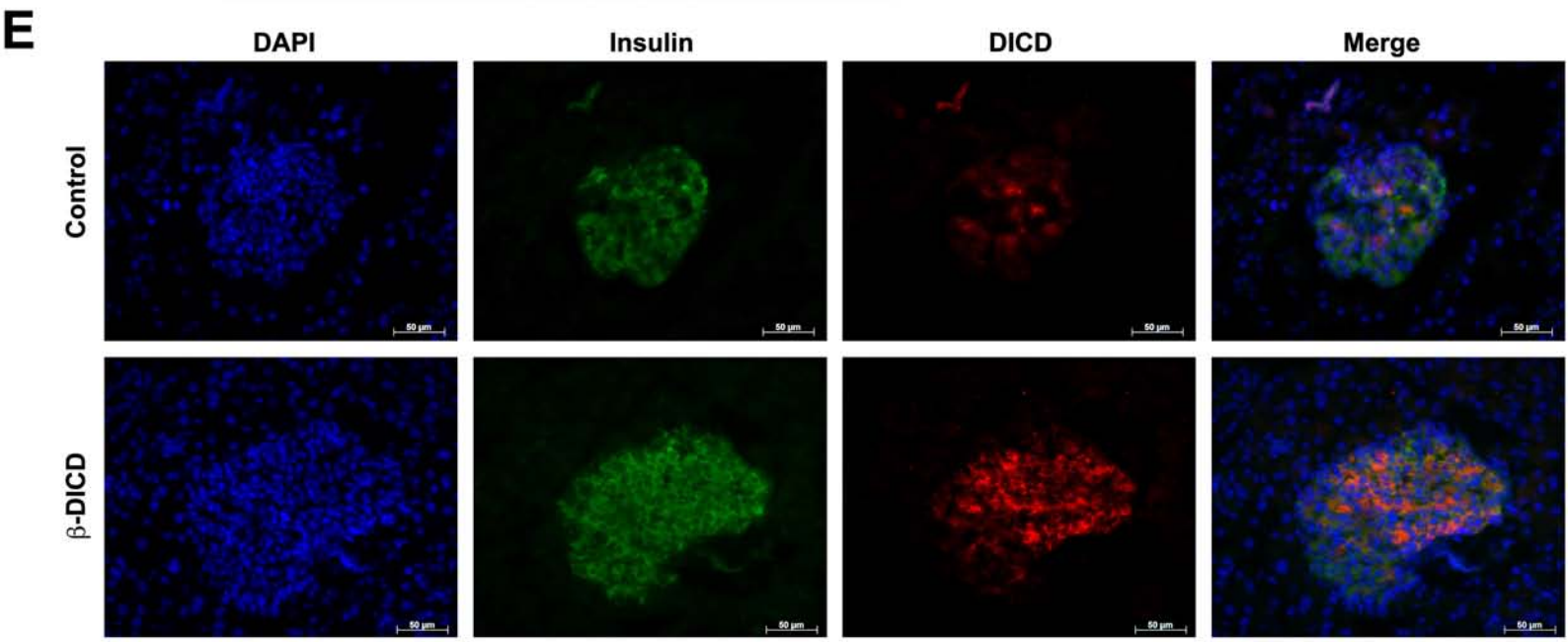

ESM Fig. 1: (**A**) DICD vector construct within the *Rosa26* locus; (**B**) *Cre*-mediated removal of the puro-stop cassette. (**C**) Gene recombination in genomic DNA (gDNA) of islets, exocrine tissue and spleen as control tissue. (**D**) Relative gene expression of *DICD* in islets of β-DICD and control mice; control n=10 and β-DICD n=11. Data are shown as mean±SD. (**E**) Co-immunostaining of insulin (green) and DICD (red) by using an antibody that specifically recognizes the DLL1 intracellular domain in pancreatic sections; n=4. Nuclei were counterstained with DAPI (blue). 8 weeks old male mice were used in the study. The scale bar represents 50 µm. Data are shown as mean ±SEM. Differences were considered statistically significant at $p<0.05$ using a two-tailed student´s t-test (**** $p<0.0001$).

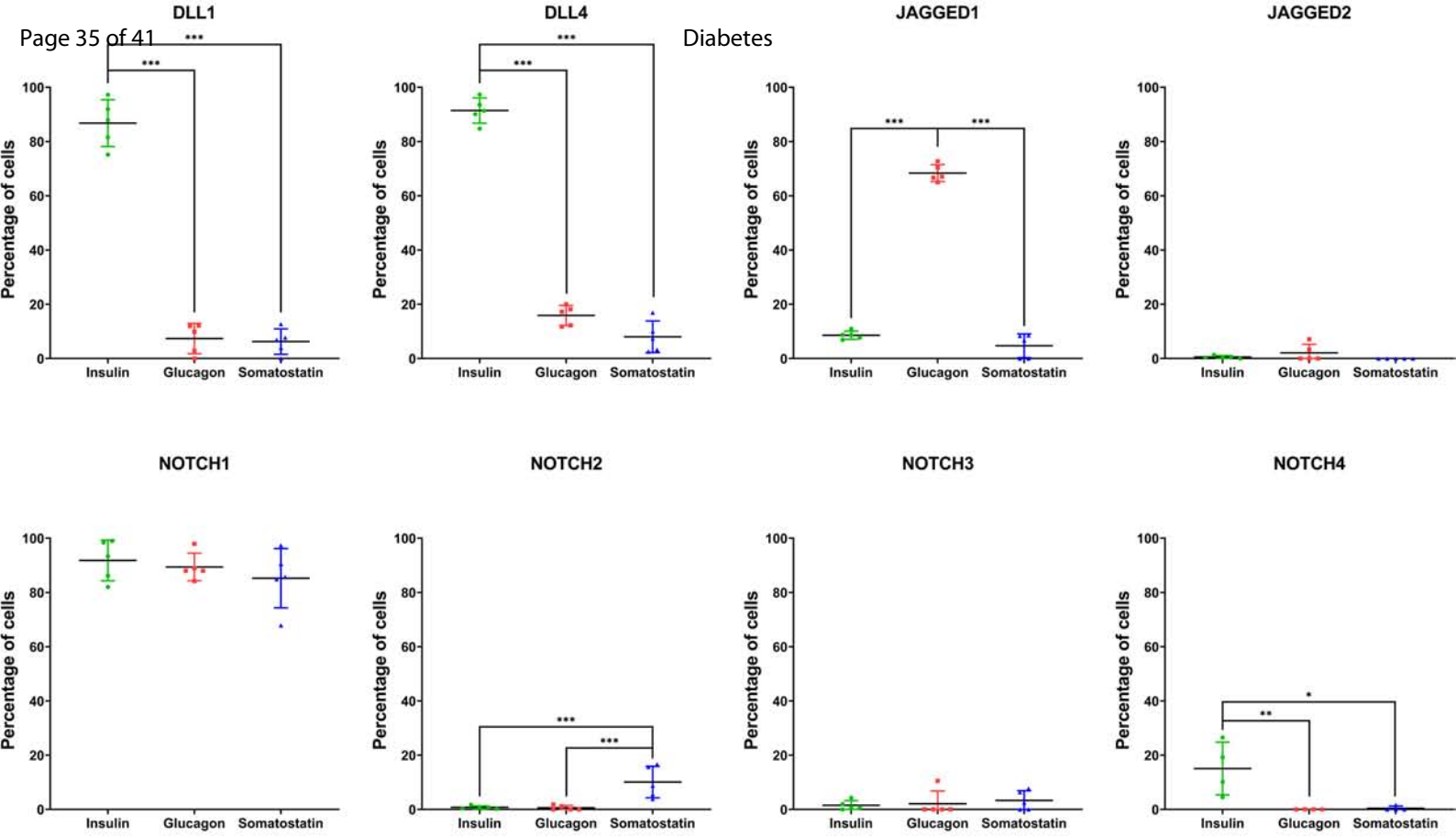

ESM Fig. 2: Quantifications displaying percentage of insulin positive β-cells, glucagon positive α-cells and somatostatin positive δ-cells expressing Notch receptors and ligands, as acquired by immunostaining of dispersed islet cells. 13-week-old male C3HeB/FeJ mice were used for this study; n=5 (NOTCH4 n=4). Data are shown as mean±SD. Differences were considered statistically significant at $p<0.05$ using a one-way ANOVA with Bonferroni *post hoc* test (**** $p<0.001$, **** $p<0.0001$).

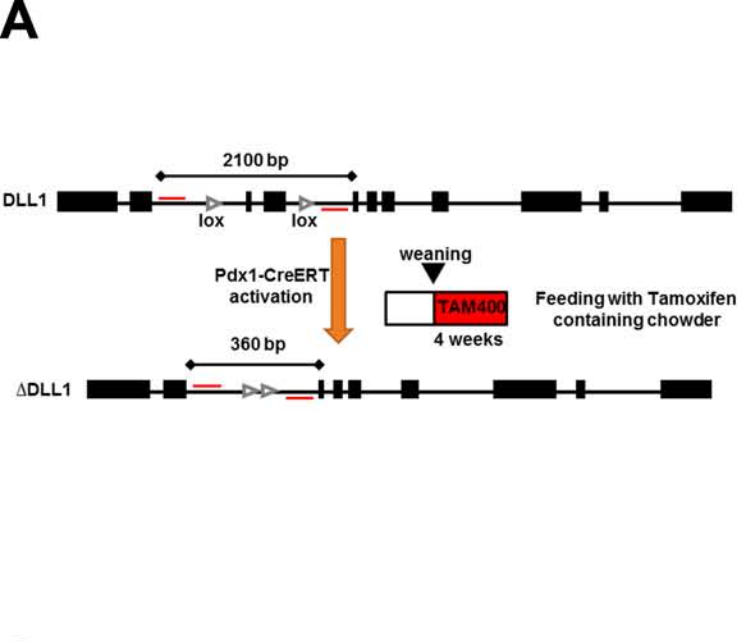

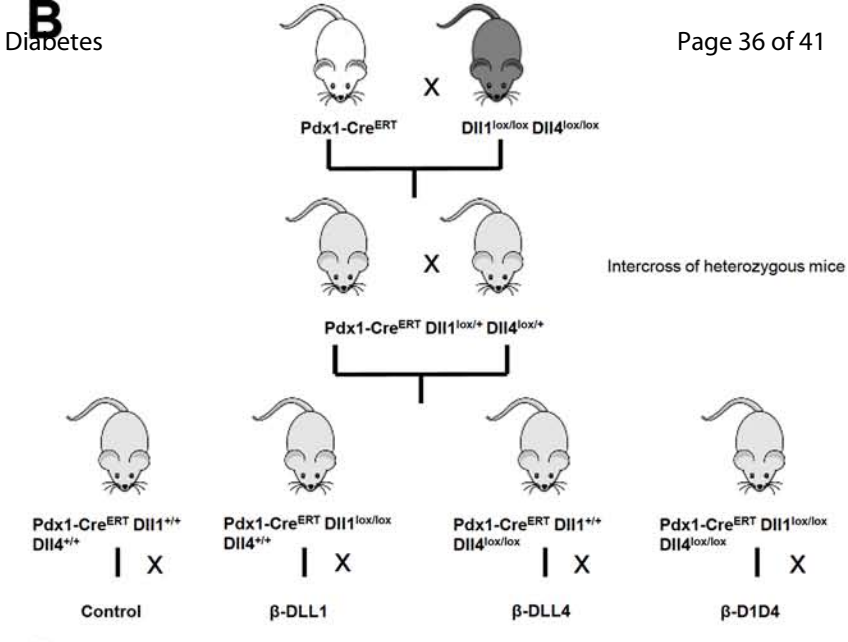

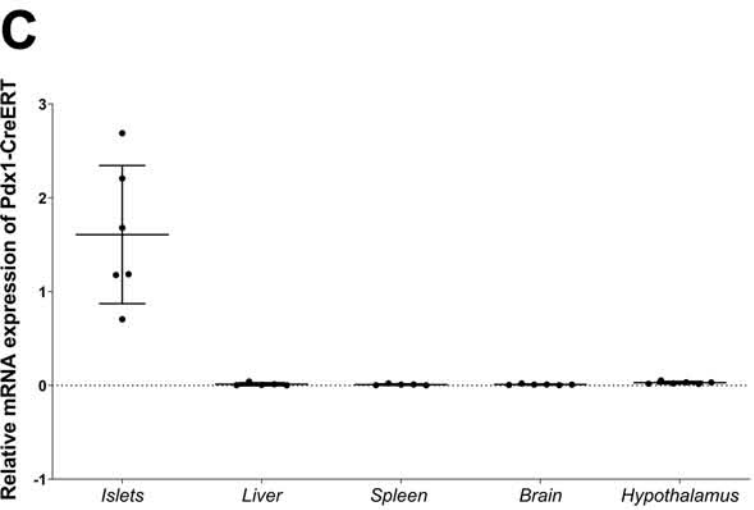

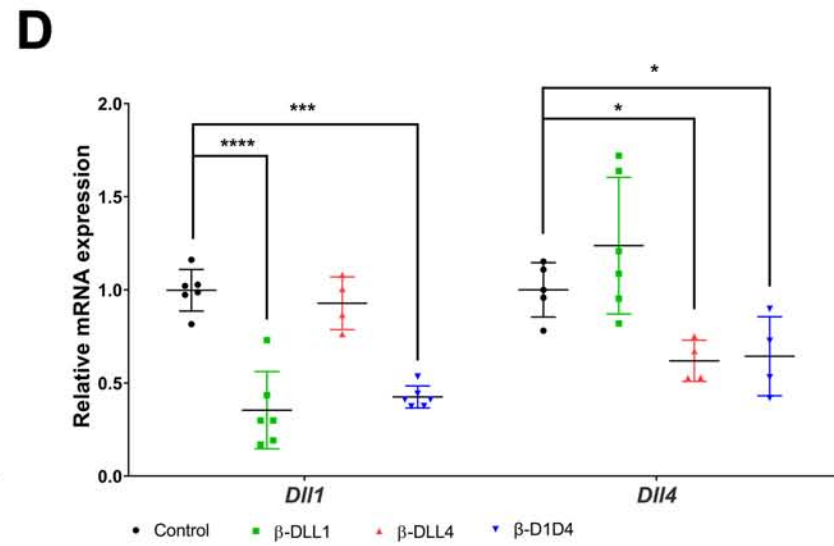

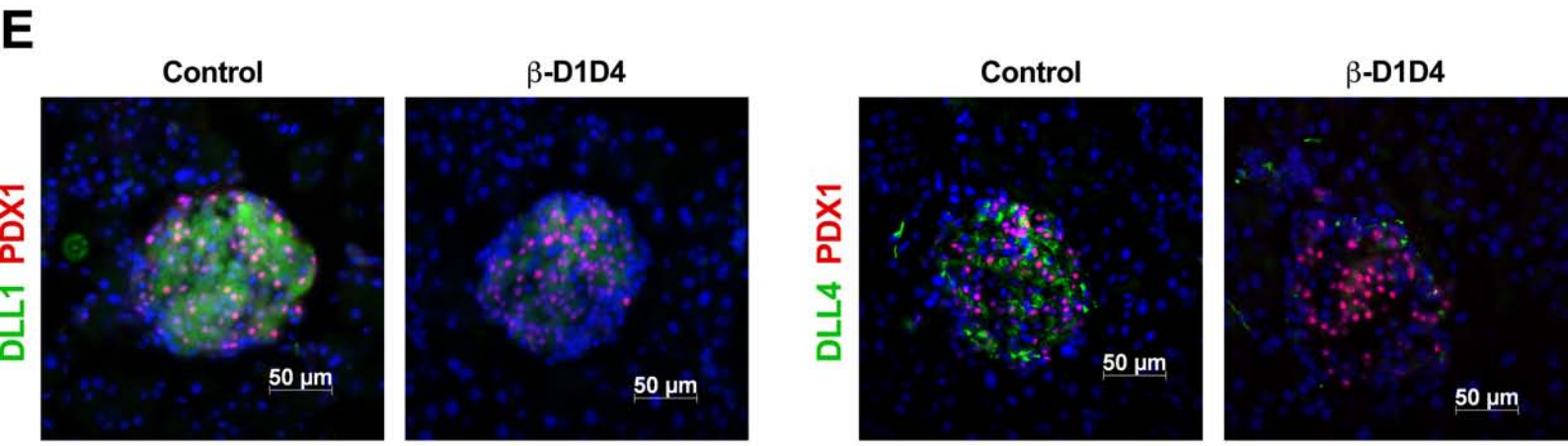

ESM Fig. 3: (**A**) Schematic representation of the *Dll1* locus and its recombination in beta-cells of the β-DLL1 mouse. Upon activation of the Pdx1-CreERT recombinase with tamoxifen, exon 3 and 4 are excised and a novel termination codon is generated. The scheme is similar for the *Dll4* locus in β-DLL4 mice. (**B**) Mating strategy to acquire four homozygous mouse lines expressing different variants of the *Dll1* and *Dll4* locus as well as Pdx1-Cre^{ERT}. (**C**) Relative gene expression of *Cre* recombinase in islets, liver, spleen, brain and hypothalamus tissue of tamoxifen-induced mice, normalized to the housekeeping gene *Hprt*; n=3. (**D**) Relative gene expression of *Dll1* and *Dll4* in islets of β-DLL1, β-DLL4, β-D1D4 and control mice, achieving 60% recombination for Dll1 and 45% for Dll4; *Dll1* control, β-DLL1 and β-D1D4 n=6 and β-DLL4 n=5; *Dll4* control n=5, β-DLL1=6, β-DLL4 and β-D1D4 n=4. (**E**) Co-immunostaining for PDX1, DLL1 and DLL4, respectively, on pancreatic sections from 8 weeks old male β-D1D4 mice; n=4. Nuclei were counterstained with DAPI (blue). The scale bar represents 50 µm. Data are shown as mean ±SD. Differences were considered statistically significant at $p<0.05$ using a two-tailed student´s t-test (* $p<0.05$, *** $p<0.001$, **** $p<0.0001$).

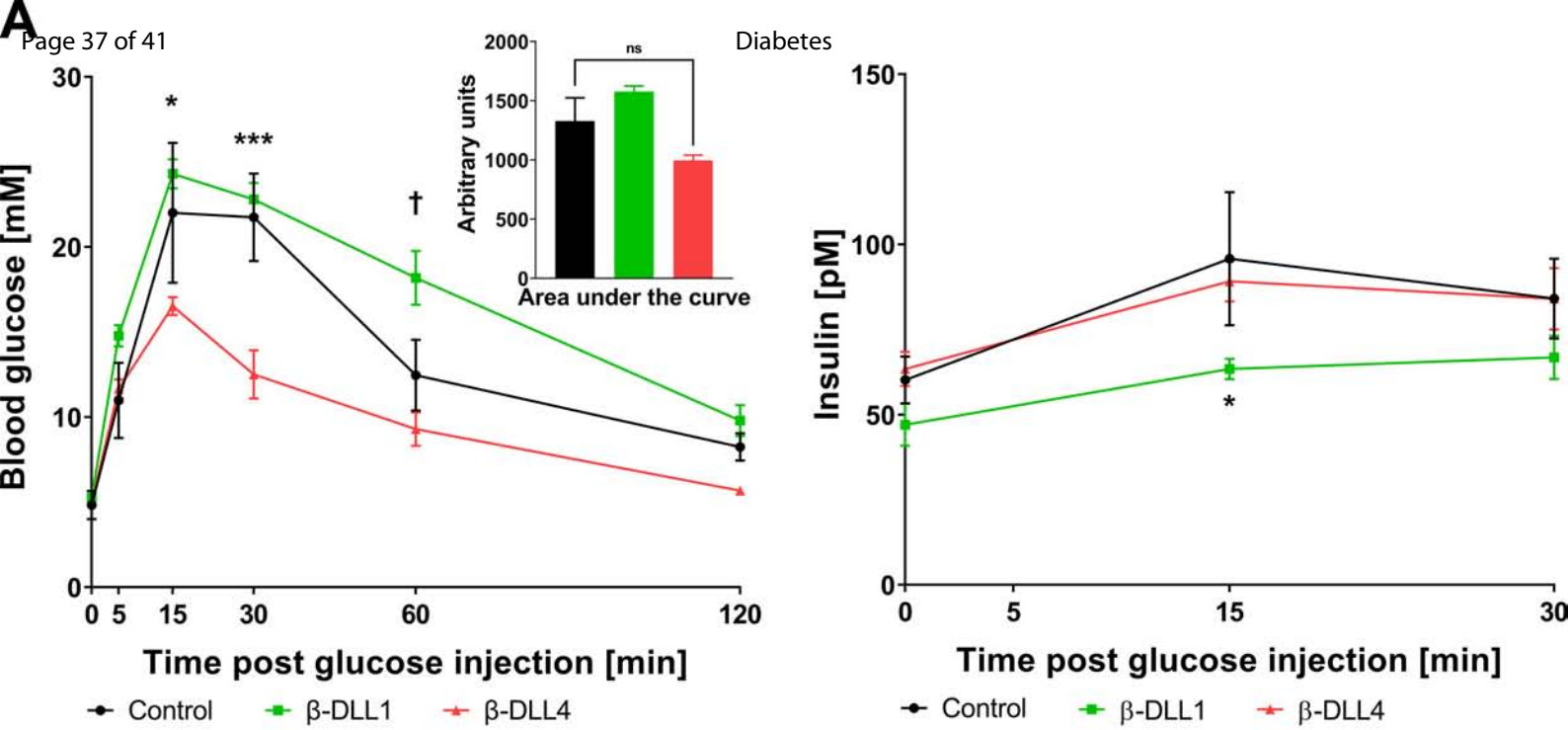

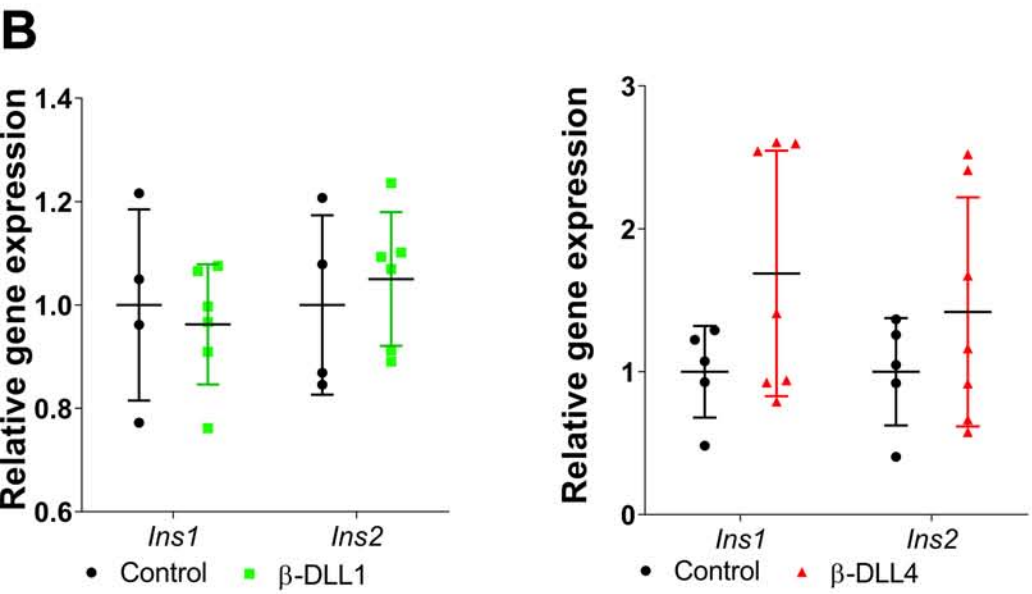

ESM Fig 4: (**A**) Measurement of blood glucose levels and insulin during an intraperitoneal glucose tolerance test in 8-10-week-old mice; control n=4, β-DLL1 and β-DLL4 n=5. (**B**) Relative gene expression levels of insulin gene isoforms in isolated islets from 8 weeks-old male; control n=4 and β-DLL1 n=6; control n=5 and β-DLL4 n=7. Data are shown as mean ±SEM for (**A**) and ±SD for (**B**). Differences were considered statistically significant at $p<0.05$ using a two-way ANOVA with Bonferroni *post hoc* test and a two-tailed student´s t-test (*, † $p<0.05$, *** $p<0.001$, †= control vs β-DLL1, *=control vs β-DLL4 and n.s – non-significant).

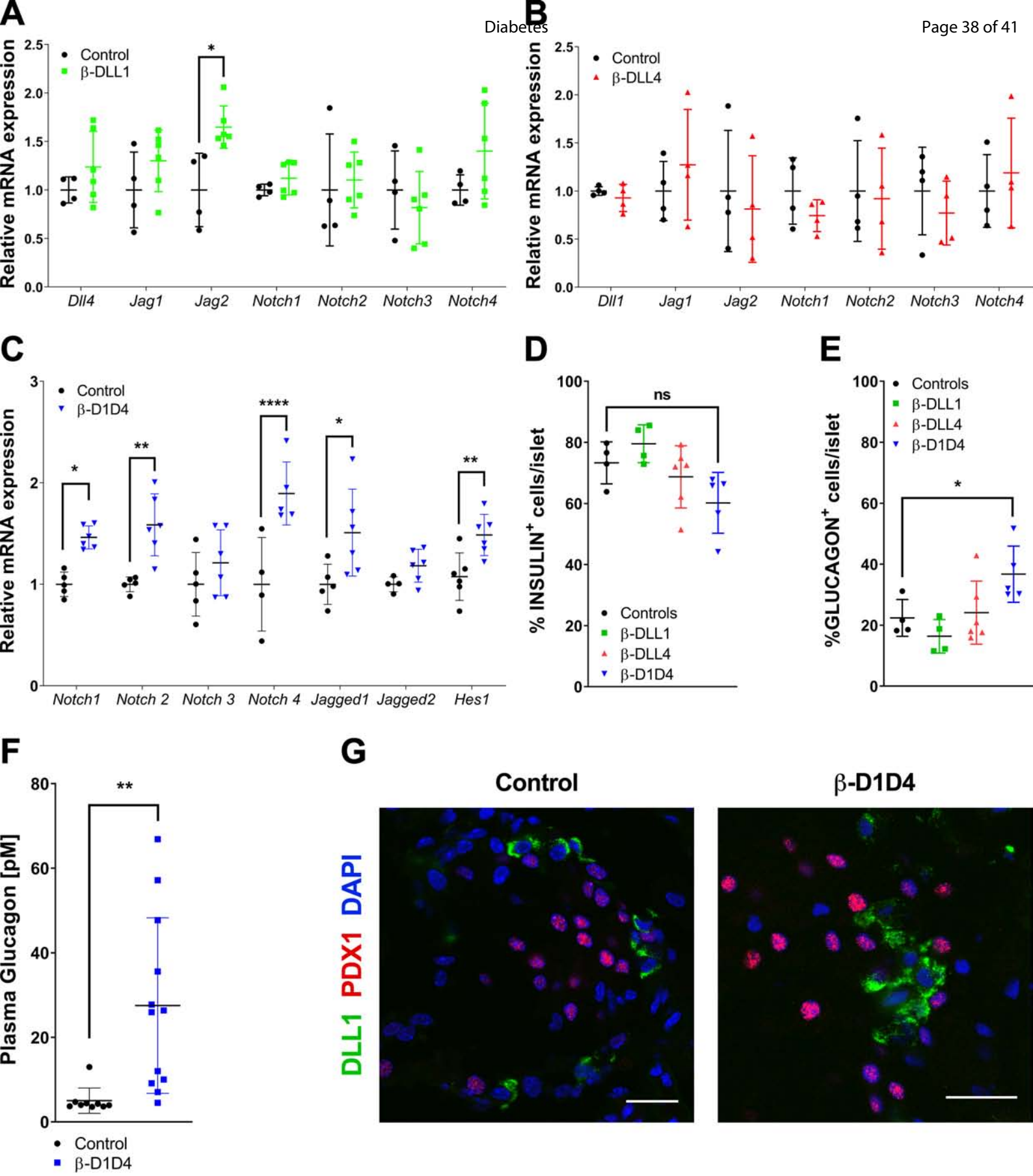

ESM Fig. 5: Relative mRNA expression of Delta-Notch components: (**A**) Control n=4 and β-DLL1 n=6; (**B**) Control and β-DLL4 n=4 and (**C**) Control n=4-5 and β-D1D4 n=6. Percentage of (**D**) insulin positive and (**E**) glucagon positive cells per islet. Control, β-DLL1 n=4, β-DLL4 n=6 and β-D1D4 n=5. (**F**) Concentration of glucagon in blood plasma: Control n=9 and β-D1D4 n=12. (**G**) Immunostaining for glucagon and PDX1; n=5. The scale bar represents 50 µm. 8-weeks-old male mice were used in the study. Data are shown as mean ±SD. Differences were considered statistically significant at $p<0.05$ using a two-tailed student´s t-test (* $p<0.05$, ** $p<0.01$, *** $p<0.001$, n.s – non-significant).

Electronic Supplementary Tables

ESM Table 1: Primer pairs used in this study

Primer for Genotyping		
Gene name	**forward primer 5´-3´**	**reverse primer 5´-3´**
DICD lox	GCACTTGCTCTCCCAAAGTC	GATACCGTCGATCCCCACT
Dll1lox	CACACCTCCTACTTACCTGA	GAGAGTACTGGATGGAGCAAG
Dll4lox	GTGCTGGGACTGTAGCCACT	TGTTAGGGATGTCGCTCTCC
Pdx1 CreERT	AACCTGGATAGTGAAACAGGGGC	TTCCATGGAGCGAACGACGAGACC
Primer for qPCR		
Gene name	**forward primer 5´-3´**	**reverse primer 5´-3´**
Cdkn1a	GCAGACCAGCCTGACAGATT	CACACAGAGTGAGGGCTAAGG
Cdkn1c	CCAATGCGAACGACTTCTT	GCCGTTAGCCTCTAAACTAACTCA
Ctgf	AGTGTGCACTGCCAAAGATG	TTCCAGTCGGTAGGCAGCTA
DICD	CACTTAGGGGTGGGGAGATT	CGCTTCCATCTTACACCTCAG
Dll1	TGGCCAGGTACCTTCTCTCT	TCTTTCTGGGTTTTCTGTTGC
Dll4	CACAGTGAGAAGCCAGAGTGTC	TCCTGCCTTATACCTCTGTGG
Glucagon	AGGCTCACAAGGCAGAAAAA	CAATGTTGTTCCGGTTCCTC
Hes1	GAGCACAGAAAGTCATCAAAG	ATGCCGGGAGCTATCTTTCT
Hes6	CCAATCTTGAGACTGAGCATTAGG	TCATAGCCAAAGTAGCAAATCTGAAC
Hey1	GAAAAGACGGAGAGGCATCA	AGCAGATCCCTGCTTCTCAA
Hey2	ATTACCCTGGGCACGCTAC	TTTTCTATGATCCCTCTCCTTTTC
Hprt	CCTAAGATGAGCGCAAGTTGAA	CCACAGGACTAGAACACCTGCTAA
Ins1	GCAAGCAGGTCATTGTTTCA	CACTTGTGGGTCCTCCACTT
Ins2	CAGCAAGCAGGAAGCCTATC	GCTCCAGTTGTGCCACTTGT
Jagged1	GCCAGACTGCAGGATAAACA	CCCTGAAACTTCATGGCACT
Jagged2	GCCAGGAAGTGGTCATATTCA	ATCCGCACCATACCTTGCTA
Mafb	TAGCGATGGCCGCGGAG	CTTCACGTCGAACTTGAGAAGG
Msln	CATCCCCAAGGATGTCAAAG	GCAGGCTTTCTGTTCTGCAT
Mtor	CAAGCAGGCAACATCTCACG	CAGAAGGGACACCAGCCAAT
Neurog3	GTCGGGAGAACTAGGATGGC	GGAGCAGTCCCTAGGTATG
Notch1	TCAGGGTGTCTTCCAGATCC	CGACTTGCCTAGGTCATCCA
Notch2	GCAGTGGATGACCATGGAA	GGTGTCTCTTCCTTATTGTCCTG
Notch3	TGCACTGGGAATGAAGAACA	CCGGCTCCTCTACCTTCAGT
Notch4	GGATAAAAGGGGAAAAACTGC	CGTCTGTTCCCTACTGTCCTG
Pdx1 Cre	TGCAACGAGTGATGAGGTTC	GCAAACGGACAGAAGCATTT
Sdha	GCAATTTCTACTCAATACCCAGTG	CTCCCTGTGCTGCAACAGTA
Smad2	GGGAGCAGAATATCGGAGGC	TGCAGAGGGCCATTCAGATG
Smad7	CTGCAACCCCCATCACCTTA	CAGCCTGCAGTTGGTTTGAG
Ubc	AGCCCAGTGTTACCACCAAG	ACCCAAGAACAAGCACAAGG

ESM Table 2: Primary antibodies used in this study

Primary antibody	Host	Clonality	Cataloge number	Company	Dilution
CRE	rabbit	polyclonal	69050-3	Millipore	1:200
Dll1 (155-173) extracellular	rabbit	polyclonal	ab10554	Abcam	1:200
Dll1 intracellular	rat	monoclonal		Gift from Dr. E. Kremmer	1:5
Dll4	rabbit	polyclonal	ab7280	Abcam	1:200
Glucagon	mouse	monoclonal	G2654	Sigma Aldrich	1:1000-1:5000
Insulin	guinea pig	polyclonal	A0564	Dako	1:200
Jagged1	rabbit	polyclonal	ab7771	Abcam	1:200
Jagged2	rabbit	polyclonal	sc-5604	Santa Cruz Biotechnology	1:50
Ki67	rabbit	monoclonal	RM-9106-S	Thermo Fisher	1:200
Mafb	rabbit	polyclonal	IHC-00351	biomol	1:200
Notch1 (immunohistochemistry)	rabbit	polyclonal	ab27526	Abcam	1:200
Notch1 (immunocytochemistry)	rabbit	polyclonal	ab8925	Abcam	1:100
Notch2	goat	polyclonal	sc-7423	Santa Cruz Biotechnology	1:200
Notch3	rabbit	polyclonal	ab23426	Abcam	1:200
Notch4	rabbit	polyclonal	N5163-100UG	Sigma Aldrich	1:200
PDX1	rabbit	monoclonal	5679	Cell Signaling	1:300
Somatostatin	rabbit	polyclonal	A0566	Dako	1:200
Somatostatin	goat	polyclonal	sc-7819	Santa Cruz Biotechnology	1:200
Somatostatin	mouse	monoclonal	14-9751-82	Affymetrix eBioscience	1:200

ESM Table 3: Secondary antibodies used in this study

Secondary antibody	Cataloge number	Company	Dilution
Alexa 488 - donkey-anti-goat	A11055	Invitrogen	1:500
Alexa 488 - donkey-anti-mouse	A21202	Invitrogen	1:500
Alexa 488 - donkey-anti-rabbit	A21206	Invitrogen	1:500
Alexa 488 - donkey-anti-rat	A21208	Invitrogen	1:500
Alexa 488 - goat-anti-guinea pig	A11073	Invitrogen	1:500
Alexa 594 - donkey-anti-goat	A11058	Invitrogen	1:500
Alexa 594 - donkey-anti-rabbit	A21207	Invitrogen	1:500
Alexa 594 - donkey-anti-mouse	A21203	Invitrogen	1:500
Alexa 594 - goat-anti-rat	ab96965	Abcam	1:500
DAPI	D9542	Sigma Aldrich	1:1000